EUROPEAN LABORATORY FOR PARTICLE PHYSICS

CERN SL/94-08 (AP)

Polarization studies at LEP in 1993

R. Assmann*, A. Blondel†, B. Dehning P. Grosse-Wiesmann, H. Grote, R. Jacobsen, J.P. Koutchouk, J. Miles, M. Placidi, R. Schmidt, J. Wenninger

Abstract

In 1993, the LEP polarization level has been increased above the target of 50% up to 57% ± 3%, demonstrating thereby that no serious depolarization from higher-order phenomena occurs at 46 GeV. Polarized beams were used to calibrate the beam energy twice a week, with an availability and reliability of 100%. In this report we describe the experiments and developments which were carried out in 1993. They aimed at obtaining polarization in close-to physics conditions and at increasing the polarization level to ensure maximum availability. For that purpose, the spin precession in the experimental solenoids was compensated by small spin rotations in the arcs. The strength of the near-by integer spin resonances was calculated directly from the closed orbit measurements, allowing their compensation and the high polarization levels obtained. The beneficial effect of the wigglers on the polarization rise-time was observed. The first evidence of a depolarization by the higher energy spread caused by the same wigglers was found in good agreement with the most recent higher-order theory and the analytical model. It gives indications on the possibility of polarization beyond 46 GeV.

Geneva, Switzerland

March 9, 1994

*Max-Planck-Institut für Physik, Werner-Heisenberg-Institut, München, Germany.

†Ecole Polytechnique, Paris, France.

Contents

1 Introduction

The polarization studies made until 1992 allowed the development of methods to obtain polarized beams, calibrate the beam energy and identify the resolution limits. The Z mass could be calibrated during these developments. The measurement of the Z width in 1993 demanded a delicate experimental method to become operational. For that purpose, LEP was carefully optimized in 1993 for polarization and performance. The physics optics was modified to maximize both performance and polarization by changing the vertical phase advance in the arc [1]. A complete vertical re-alignment of the machine was predicted to be very effective for polarization [2] and carried out. Furthermore the accuracy of the beam monitors was much improved. These provisions were expected to allow a higher 'natural' polarization and the ability to implement efficiently methods which had been shown in simulation to improve the polarization degree. A further requirement was to obtain polarization in conditions as close as possible to physics, so as to avoid an hypothesis on the energy dependence on the optics. To speed-up operation with polarized beams, the polarimeter hardware and software were upgraded. This report summarizes the progress and the observations in the field of polarimetry and polarization dynamics, which gives some insight as to the possibility of polarizing the beams at energies higher than 46 GeV.

2 Polarimetry

2.1 Principle

The beam polarization is measured with a Compton polarimeter [3]. The cross section for the Compton scattering of photons on polarized electrons depends on the polarization of both photons and electrons. A selectable electron bunch is illuminated with a high intensity circularly polarized light pulse from a Nd-YAG laser operating at 100 Hz (multi-photon measurement). Reversing regularly the helicity of the circularly polarized light results in two different distributions of backscattered photons with a vertical center-of-gravity shift Δy which is proportional to the transverse beam polarization P:

$$\Delta y = \xi \cdot P \tag{1}$$

The polarization scale factor ξ is determined from simulations and measurements. The distributions of backscattered photons are measured separately for both helicities with a 2 mm pitch silicon strip photon detector. The polarimeter was originally constructed for polarization measurements on electrons. In 1993 a simple extension was installed in order to make polarization measurements also possible for positrons. A schematic view of the extended LEP polarimeter is shown in fig. 1. Essentially the installation of one additional mirror allows head on Compton scattering of the photons on the positron beam. Backscattered photons from positrons are detected with a second detector. A first prototype measurement of positron beam polarization was performed. More details on the LEP polarimeter can be found in [4].

An example for the measured average distribution and the measured asymmetry between the two helicities is shown on fig. 2 for a polarization degree of more than 50% measured on electrons. The center-of-gravity shift Δy is calculated by cross-correlating the two measured distributions [5].

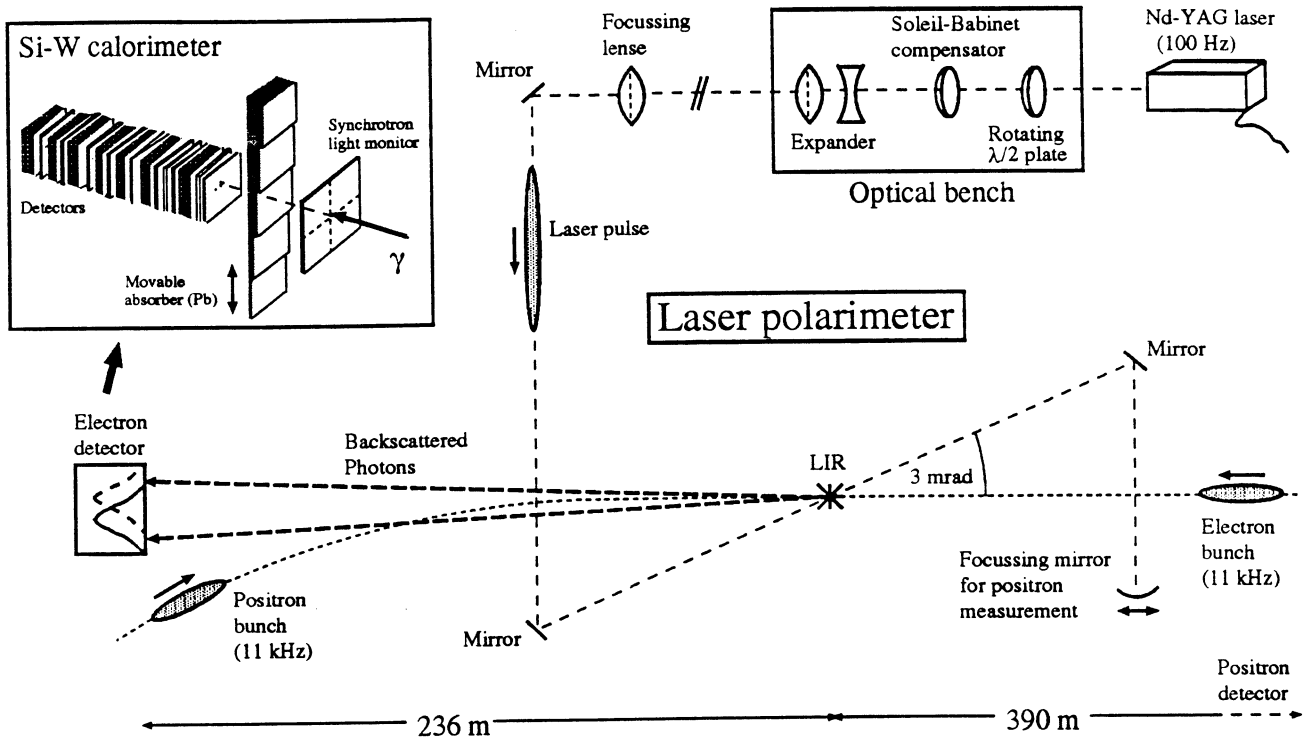

Figure 1: *Schematic view of the LEP polarimeter. A Nd-YAG laser in the optical lab generates high intensity light pulses with a repetition rate of 100 Hz. The light is circularly polarized with alternating helicity by a rotating $\lambda/2$ plate and a Soleil-Babinet compensator. The polarized light is then transported over 114 m into the LEP tunnel and into the beam pipe where it is brought into collision with an electron bunch (LIR). In order to get an optimum interaction rate the focus of the laser beam is adjusted to be at the LIR. The backscattered photons from electrons are detected in a Si-W calorimeter. The difference in the measured vertical γ-distributions yields the polarization signal. With a movable mirror the laser light can be reflected back into the beam pipe and can be brought into collision with a positron bunch. With a second detector backscattered photons from positrons can be measured.*

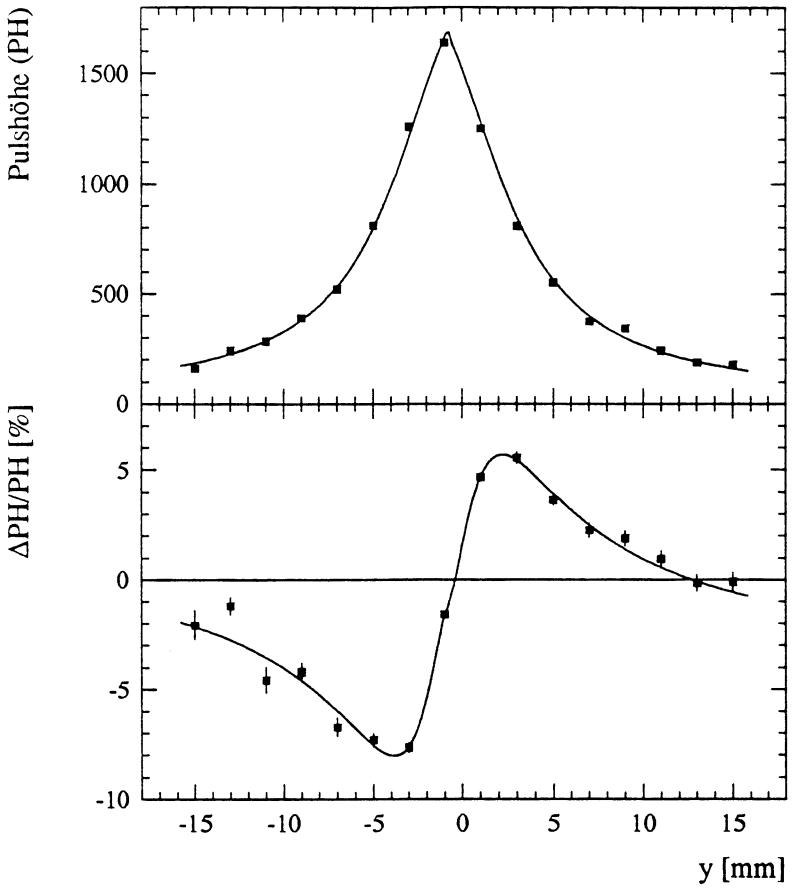

Figure 2: *Top: Pulse height (PH) versus the vertical position y as measured in the 2 mm pitch silicon strip photon detector at LEP. The distributions of backscattered photons for the two helicities are averaged. Bottom: Measured difference between the distributions of backscattered photons with positive and negative light helicities (asymmetry). The beam polarization is here about 57%.*

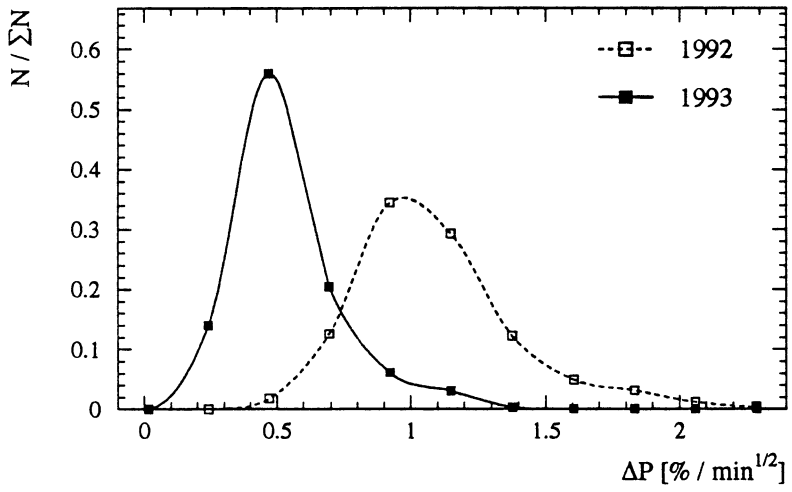

Figure 3: *Distributions of statistical errors ΔP which were achieved in 1 minute measurements with the LEP polarimeter in 1992 and 1993.*

2.2 Performance of the polarimeter in 1993

The accuracy of the polarization measurement is mainly determined by the number of backscattered photons (statistical error), the time stability of the photon-electron overlap and the quality of light polarization (systematic offset errors). In order to improve the accuracy of the LEP polarimeter and to facilitate its operation a new laser was installed for the 1993 run period. The laser repetition rate went from 30 Hz to 100 Hz and the number of photons per shot from $2.45 \cdot 10^{17}$ (90 mJ) to $3.26 \cdot 10^{17}$ (125 mJ). An improvement in statistics by a factor 4.4 was expected from this. A better laser focus at the interaction point further increased the statistics and in total up to 10 times more backscattered photons were expected [6]. In fig. 3 the distributions of measured statistical errors are compared for one experiment in 1992 and one in 1993. The observed improvement in the statistical errors corresponds to about 5 times more backscattered photons. The factor of 2 which is missing is attributed to a horizontal instability of the laser beam position at the LIR. Tiny low-frequency vibrations of the vacuum chamber have been identified, causing the mirrors in the beam pipe and the laser beam to move. The mechanical stability of the chamber is being improved. The laser-beam luminosity was in any case close to the possible limit: it was noticed that the electron beam lifetime was limited by Compton scattering to 3 to 6 hours. The luminosity depends on the set-up of the polarimeter and the tuning of the overlap in the photon-electron interaction region. A feedback steering system was installed close to the end of 1993 in order to achieve this high performance regularly and to maintain it over long periods.

The limited aperture of the backscattered γ beam line in combination with changes in position and shape of the γ distributions leads to systematic errors in the polarization measurement [7]. If the back-scattered photon beam is not very well centered with respect to the aperture, the cut of the distributions are asymmetrical when reversing the light helicity. This leads to a spurious center-of-gravity shift which is not related to beam polarization. It was shown in [7] that the spurious linear component in the circularly polarized laser light contributes as well to the bias. To evaluate the typical magnitude of the systematic offset error an experiment with a well measured rise of the polarization is investigated. The analysis is restricted to data with positions of the distributions of backscattered photons centered on the detector within 1.5 mm horizontally and 0.8 mm vertically. This corresponds to typical good running conditions of the polarimeter. The rise of polarization is fitted and the RMS-deviation of the measurement from the fitted value is taken as the total measurement error ΔP_{tot}. The discrepancy between ΔP_{tot} and the average statistical error ΔP_{stat} is explained by a systematic offset error ΔP_{syst}. Including the error $\Delta P_{\mathrm{scale}}$ from the determination of the polarization scale (see next section) the error on the polarization measurement is:

$$\Delta P_{\mathrm{tot}} = 0.8\,\% + \Delta P_{\mathrm{scale}} \qquad \text{(total error in 1 minute)} \tag{2}$$

$$\Delta P_{\mathrm{stat}} = 0.6\,\%\,\mathrm{min}^{-\frac{1}{2}} \qquad \text{(statistical error)} \tag{3}$$

$$\Delta P_{\mathrm{syst}} = 0.5\,\% \qquad \text{(systematic offset error)} \tag{4}$$

$$\Delta P_{\mathrm{scale}} = 0.048 \cdot P \qquad \text{(polarization scale error)} \tag{5}$$

The value given for the systematic offset error must be interpreted in the following way: if the position of the recoil photon beam is kept within 1.5 mm horizontally and 0.8 mm vertically around the center of the detector an average systematic error of 0.5% is achieved. The actual systematic offset error, however, depends on the actual positions and eventually on the light polarization and increases with a worsening positioning. Since the steering of the polarimeter is

complex, its working point was not always kept to its optimum when other tasks had priority. Therefore larger systematic offset errors can be found in the data. If the positions are off by several mm the systematic offset error can reach several %. A feedback steering system for the automatic control of the positions of the recoil beam on the detector was installed in autumn 1993. The first experience with its operation shows that systematic offset errors can easily be kept below 1%.

In 1991 a fast network data transfer of the polarimeter data to the LEP control room and an upgraded online data processing was implemented. Measurements could be accessed in real time over a graphical interface thus giving a fast response of the polarization signal to any change in the storage ring. This is a condition for energy calibration with resonant depolarization. Remote control of important parameters of the polarimeter allowed to maintain a good data quality. In 1992 data acquisition and data processing were further improved and in the beginning of 1993 the LEP polarimeter had become fully remote controllable. The goal to facilitate the operation of the polarimeter was achieved and led to a significant reduction in set-up time in 1993.

2.3 Calibration of the polarization scale

The relative accuracy of polarization measurements is dominated by systematic offset errors caused by the limited aperture and time dependent changes in the electron-photon overlap region. However, the error on the absolute degree of polarization is dominated by the error on the polarization scale if the polarization is higher than 30%. The polarization scale factor ξ, which was defined in eq. 1, can be determined from simulations where it comes out for the electrons to be:

$$\xi_{\text{sim}} = (5.4 \pm 1.0)\,\mu\text{m}/\% \tag{6}$$

ξ can also be determined from the measurement of the build-up time. With the initial condition $P = 0$ at $t = 0$ the build-up of beam polarization P to P_∞ is given by:

$$P = \frac{92.4\%}{1 + \frac{\tau_p}{\tau_d}} \cdot \left(1 - \exp\left(-t/\tau_p^{\text{eff}}\right)\right) \tag{7}$$

$$= \underbrace{\frac{\tau_p^{\text{eff}}}{\tau_p} \cdot 92.4\%}_{=\Delta y_\infty/\xi} \cdot \left(1 - \exp\left(-t/\tau_p^{\text{eff}}\right)\right) \tag{8}$$

The effective polarization build-up time τ_p^{eff} is defined as $(\tau_p^{\text{eff}})^{-1} = \tau_p^{-1} + \tau_d^{-1}$. The polarization time τ_p is determined by the configuration of the magnetic bending fields and the spin tune ν while τ_d is the depolarization time. For LEP we find:

$$\tau_p = \frac{6.31 \text{ hours}}{(\nu/100)^5} = \begin{cases} 5\text{ h }52\text{ min} & \text{with } \nu = 101.5, \\ 5\text{ h }19\text{ min} & \text{with } \nu = 103.5, \\ 4\text{ h }50\text{ min} & \text{with } \nu = 105.5. \end{cases} \tag{9}$$

A careful measurement of the polarization rise-time τ_p^{eff} and of the asymptotic mean shift Δy_∞ yields the polarization scale factor ξ using equation 7: A fit to the measured mean shifts yields the effective build-up time τ_p^{eff} and the asymptotic mean shift Δy_∞. With the well known τ_p the asymptotic polarization P_∞ in % can be calculated from τ_p^{eff}. The best fit from 1993 yields:

$$\xi_{\text{exp}} = (4.36 \pm 0.21)\,\mu\text{m}/\% \tag{10}$$

This value of ξ agrees within the errors with the result from simulations and with results from former years. It is confirmed in 1993 by another experimental result yielding $\xi_{exp} = (4.16 \pm 0.40)\ \mu m/\%$. For the analysis we take the best measurement of ξ and use a value of $4.36\ \mu m/\%$. Absolute scale errors are not included in the errors given in the figures.

2.4 Data analysis

The data which will be presented in the following were often taken during ongoing energy calibrations. With high beam polarization, energy calibration by resonant depolarization is not disturbed by small systematic offset errors of a few percent. Therefore the tuning of the LEP polarimeter was not always kept at the optimum. To exclude extreme effects a cut of ± 3.5 mm on the horizontal position and a cut of ± 1.5 mm on the vertical position was used for the data analysis. In practice only a few measurements during the set-up of the polarimeter are discarded with these cuts. The systematic offset error in the data presented is typically of the order of 1-2%. However, during the experiment when maximum polarization was measured (see fig. 15) the strongly drifting orbit of the electrons caused much larger offset errors which went up to about 6% in the beginning of the experiment. Later on with maximum polarization the systematic offset error was measured to be 0.9% and was corrected. Often only one or two monitor bunches were used to observe the rise of polarization. The other bunches were depolarized for energy calibration in the meantime. Polarization measurements for energy calibration on these bunches are generally left out for reasons of clarity. This explains time intervals in the figures without any measurements.

3 Polarization in physics conditions

3.1 Spin matching of solenoids

The experimental solenoids have very strong longitudinal magnetic fields and the resulting spin rotation around the longitudinal axis (ALEPH: 66 mrad) must be compensated in order to obtain polarization. The spin matching of all experimental solenoids in LEP was an important goal for 1993 because energy calibration at the end of physics coasts needs polarization with the experimental solenoids on. The spin compensation of the ALEPH solenoid was already demonstrated in 1992 [8]. As the solenoid fields are well known the resulting spin rotations can be calculated and compensated to a good accuracy by a configuration of vertical orbit bumps close to the solenoids [9]. The principle of the solenoid spin matching is illustrated in fig. 4. Essentially a closed bump of spin is implemented around the solenoid.

The two first polarization fills in 1993 were used to spin match all four experimental solenoids (ALEPH, DELPHI, OPAL, L3) with the theoretically calculated compensations. In fig. 5 the depolarizing effect of the ALEPH solenoid and the spin matching of ALEPH and DELPHI is shown. The spin matching of OPAL and L3 is shown in fig. 6. Some loss of polarization was observed after spin matching, either related to an inaccuracy of the solenoid model or to side effects such as orbit and tune perturbations. The fact that much higher polarization levels could be reached later with solenoids shows that the former loss must have been due to side effects of the solenoids or compensation. The theoretical limit on polarization from the solenoid spin matching is 72.6% [9].

It was noticed that the solenoid spin matching bumps produce significant betatron coupling. The bump configuration used is optimized to create a small vertical orbit excursion and no extra vertical dispersion. However, the condition for no extra vertical dispersion is orthogonal to the

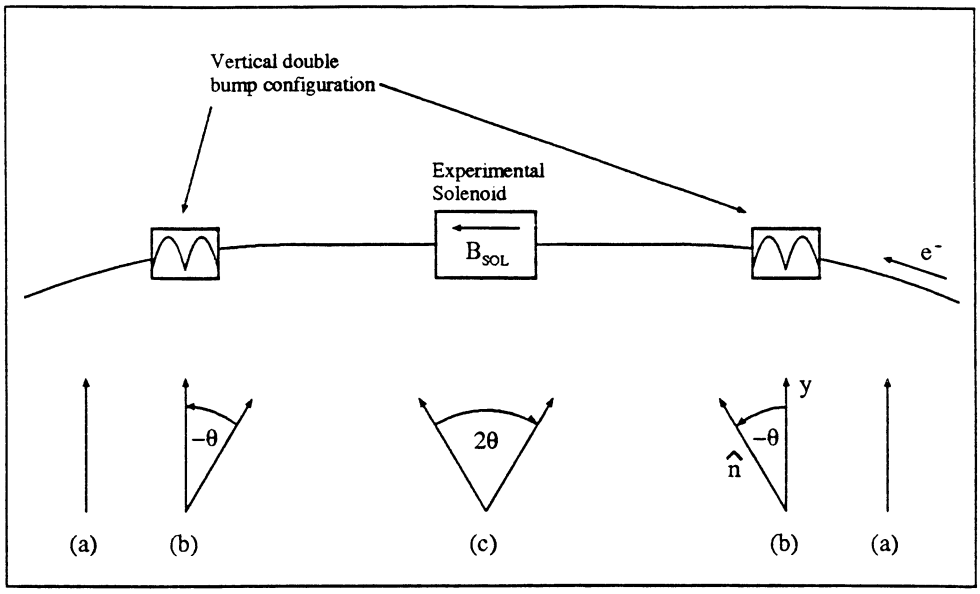

Figure 4: *Principle of solenoid spin matching. The longitudinal B-field of the experimental solenoid rotates the spin by an angle of 2θ around the longitudinal axis (c). Vertical closed orbit bumps at the beginning of the arcs on both sides of the experiment compensate the spin rotation (b) so that the $\vec{n}_0$-axis (spin precession axis on the closed orbit) is vertical almost everywhere in the arcs (a).*

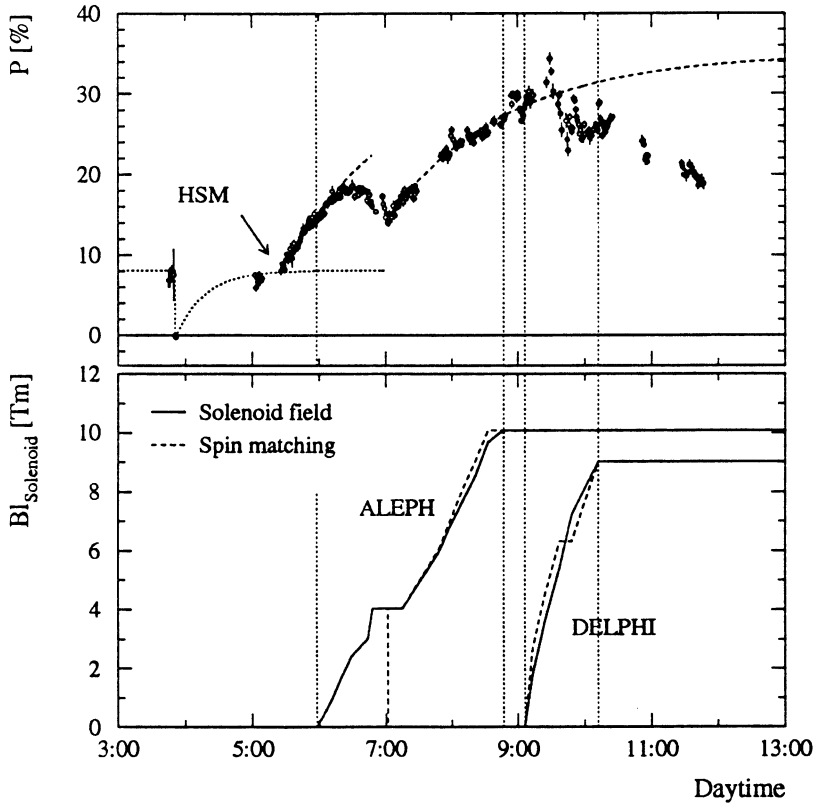

Figure 5: *The first experiment in 1993 is shown. The polarization could be increased from 8% to above 30% by deterministic Harmonic Spin Matching (HSM). The depolarizing effect of the unmatched ALEPH solenoid and the spin matching of ALEPH and DELPHI is shown. After spin matching some loss in polarization can be observed. The spin tune (beam energy) was 105.5 during that experiment.*

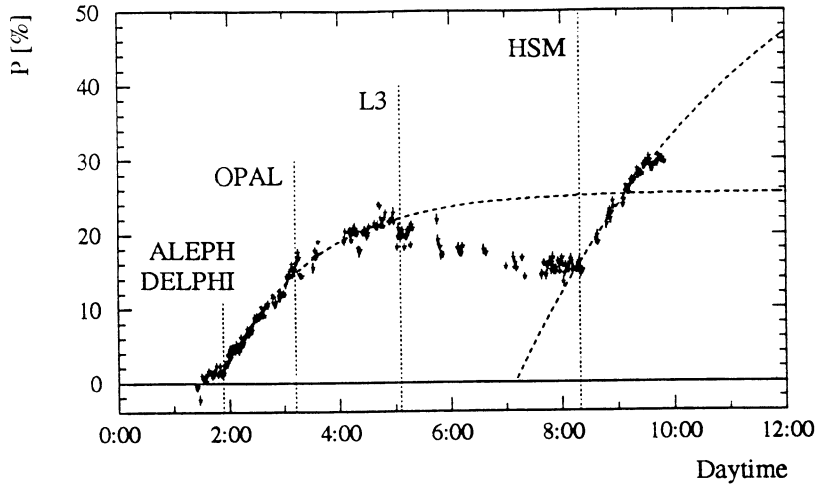

Figure 6: *Spin matching of OPAL and L3. They have been compensated in the same way as shown in fig. 5 for ALEPH and DELPHI. After the spin matching of L3 polarization dropped and could only be recovered after deterministic Harmonic Spin Matching (HSM). The spin tune was at about 101.5 during the experiment.*

condition for no extra betatron coupling. It was decided to accept additional betatron coupling which was corrected with skew quadrupoles.

3.2 Squeezed optics

In a squeezed optics with large β in the insertion doublet an instability of the vertical orbit and higher dispersion with a symmetry of four is potentially produced. The vertical dispersion may excite systematic Q_y spin resonances and lead to depolarization. This effect can be minimized taking advantage of the high quality closed orbit surveillance and correction. During one fill the beam was squeezed from $\beta_y^* = 21$ cm down to $\beta_y^* = 7$ cm whilst polarization was monitored. No loss in polarization was observed. Furthermore on three occasions polarization experiments were performed with a β_y^* of 5 cm. Since polarization levels up to 30% with higher asymptotic values have been observed in this condition it is clear that the squeezed optics is not a serious problem but is more demanding for machine stability.

3.3 Pretzel scheme

The LEP pretzel scheme used for physics [10] causes the beams to be horizontally separated in the arcs and in the odd interaction points. In a perfect machine, it should have no influence on spin dynamics except for a slight spin tune shift verified to be negligible ($-.2 \pm .4$MeV was found experimentally). The energy calibrations were nevertheless carried out with the pretzel scheme since the polarization level was sufficient. Yet, it never reached the high levels obtained without the pretzel scheme and was significantly different at the three energy levels explored (section 3.5). Two side effects of the pretzel scheme may explain the observations.

- The vertical bumps used to compensate the solenoids are perturbed by the pretzel scheme and are not closed anymore. This widens the systematic spin resonances.
- Due to the residual skew quadrupole in the dipoles, the pretzel orbit couples to the vertical plane with a symmetry of 4. This again excites systematic resonances.

This would explain the lower polarization at 103.5 and 105.5 as compared to 101.5: $106 = Q_x + 2{\cdot}8$ and $104 = Q_y + 7{\cdot}4$. The importance of systematic integer spin resonances is shown in fig. 17

and is discussed in more detail in [11]. A spin tune 101.5 is safe with respect to systematic integer spin resonances and is expected to yield the best polarization.

If necessary, it should be possible to minimize the first source by using different bumps for the solenoid compensation. The minimization of the second effect, which is different for the two beams, seems difficult.

3.4 Effect of betatron tunes on polarization

Depolarization is strongly enhanced when a resonance condition occurs between the spin precession and betatron and/or synchrotron oscillations. For the polarization studies, the tunes were optimized to avoid the strongest spin resonances following the principles discussed in [12]. On the 90/60 lattice used at LEP in 1993 the synchrotron tune is lower, resulting in the following values for the optimal tunes: $Q_x = 90.10$ and $Q_y = 76.20$. The value of the synchrotron tune Q_s is determined to a large extent by the available RF-voltage and the quantum lifetime of the beam. It is fine adjusted such that the Q_s satellites from the integer spin resonance $k_0 + 1$ above the spin tune fall on top of the Q_s satellites from the integer spin resonance k_0 below the spin tune:

$$k_0 + k_s Q_s = k_0 + 1 - k'_s Q_s \tag{11}$$

This condition is fulfilled for a synchrotron tune Q_s of 0.0625 close to the value used for physics (0.065). The given tunes are referred to as the polarization tunes.

The horizontal tune differs very much from that used in physics coasts ($Q_x = 90.26$ typically). During two experiments it could be shown that on physics tunes, in particular with a high Q_x, large depolarization occurs. In fig. 7 polarization is compared for physics settings and polarization settings. With physics tunes a degree of only 9% polarization was observed. After the tunes were changed to their standard settings polarization improved to almost 30% with a much higher asymptotic value. The degree of polarization with physics tunes could not be improved by deterministic Harmonic Spin Matching. This technique, as will be discussed later, reduces efficiently the spin resonances driven by a tilt of the vector $\vec{n}_0$. $\vec{n}_0$ is the spin closed solution on the closed orbit. Obviously the limiting spin resonance close to physics tunes is driven by another mechanism.

A more systematic study of the effect of betatron tunes on polarization is shown in fig. 8. With 20% of polarization (still rising) the tunes were changed to physics tunes and polarization decreased to 8-10%. Small changes in Q_x and Q_y could not re-establish high polarization. Only when the fractional part of Q_x was lowered to 0.25 the degree of polarization recovered up to 16% with a higher asymptotic value. However, the asymptotic degree of polarization calculated from a fit turns out to be smaller than with polarization tunes (27% instead of 46%).

There are two possible conclusions from these results. Since Q_x is significantly higher in physics conditions, synchrotron satellites of the linear Q_x spin resonances are of lower order close to the half integer and are therefore much stronger. This may cause depolarization. A more probable cause for the observed depolarization is the $Q_x + Q_y$ non-linear spin resonance which would be expected at a spin tune of ≈ 101.48 for the physics tunes. This is very close to the actual spin tune which was ≈ 101.465, and coincides when taking into account the coherent detuning. The $Q_x + Q_y$ spin resonance is driven by orbit deviations in the sextupoles.

Advantage was taken from the polarized beam at the physics tunes to measure a possible dependence of the beam energy on the fractional tunes. No energy difference was found between the physics and polarization tunes. All the other experiments and energy calibrations were therefore carried out on the polarization tunes.

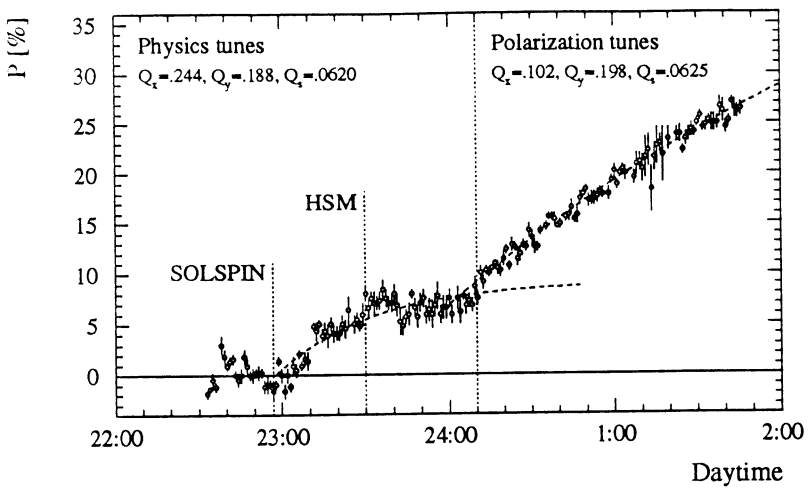

Figure 7: *Polarization is shown for two different settings of tunes. With "physics tunes" polarization rose to about 9% after spin matching of the solenoids (SOLSPIN). Harmonic Spin Matching of the vertical closed orbit (HSM) could not improve the polarization. After shifting the tunes to the polarization settings polarization rose to 30%.*

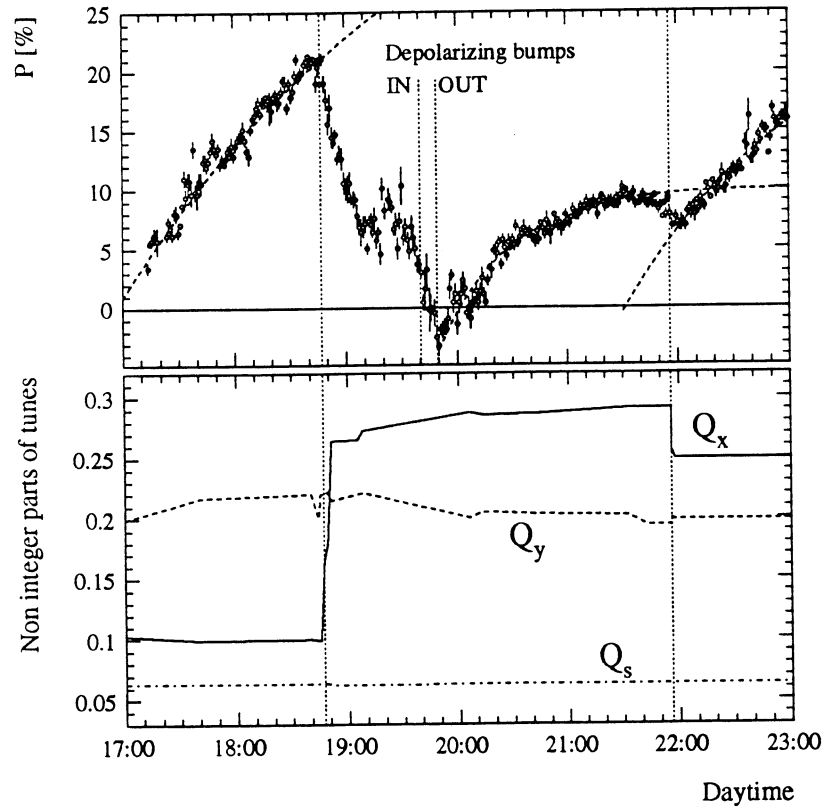

Figure 8: *Polarization is shown for different tunes Q_x, Q_y and Q_s. In the beginning polarization above 20% was achieved with polarization tunes. After changing essentially Q_x close to its value in physics coasts polarization degraded to about 8%. The beam was depolarized and the build-up of polarization was measured. When changing Q_x to some other calculated optimum point high polarization came back with a somewhat smaller asymptotic value.*

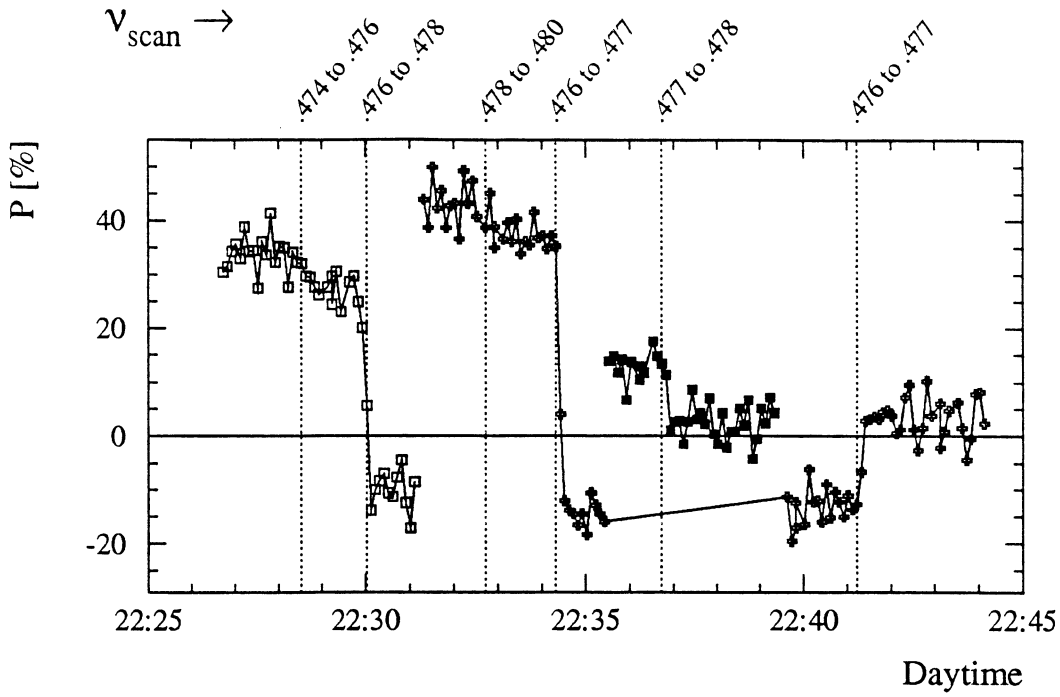

Figure 9: *Example of energy calibration. Several bunches are used to measure the fractional part of the spin tune. A partial spin flip to negative polarization was observed and checked by flipping it again.*

3.5 Observations during energy calibrations

Energy calibration was performed roughly twice a week on off-peak fills and twice in 1993 on Z-peak energy. After physics conditions were ended a standard procedure for polarization setup was followed. On most occasions the positron beam was dumped. Then the tunes were changed from physics settings to polarization settings and the closed orbit was well corrected. After that deterministic Harmonic Spin Matching was applied on the vertical closed orbit and finally the solenoids were spin matched. In parallel the polarimeter was set up.

During energy calibration runs polarization of about 10% was found on the Z-peak at 45.6 GeV ($\nu = 103.5$) and at 46.5 GeV ($\nu = 105.5$). Transverse polarization above 25% was found at 44.7 GeV ($\nu = 101.5$) during energy calibration. Polarization was generally smaller than in polarization experiments. In addition the measured polarization was smaller for spin tunes of 103.5 and 105.5 than for 101.5. The main difference between dedicated polarization experiments and standard energy calibrations is the squeezed optics and the horizontal Pretzel scheme. A possible explanation for the different polarization levels observed was given in section 3.3. Fig. 9 shows an example of energy calibration. More details on the accuracy and on the results of energy calibration by resonant depolarization for LEP in 1993 can be found in [13].

4 Increasing the polarization level

It was shown how important it is to locate the spin tune and hence the beam energy far from spin resonances. The second step is to compensate or weaken as far as possible the depolarizing resonances. The provisions to minimize their strength by tight alignment and optics design were detailed in [1]. In 1993, we implemented in addition spin resonance compensation, known as Harmonic Spin Matching (HSM).

4.1 Principle of spin matching

Here, we recall briefly the essential results of the theory of the spin motion in the approximation of small amplitude oscillations (see e.g. [14]). The motion of the classical spin vector $\vec{S}$ of an electron in a magnetic field $\vec{B}$ is a precession about $\vec{B}$. In an ideal flat ring, all the spins precess around the vertical guide field. In a real accelerator with imperfections causing the beam to go off-axis vertically, spurious rotations, mainly occurring in the quadrupoles, bend the spin away from the vertical. The spins appear then to precess about an inclined axis $\vec{n}_0(s)$ which varies along the closed orbit. This axis is the real eigenvector of the one-turn transport of the spin. It is equally the stable spin direction; spin components along any other direction will be diluted due to quantum excitation. The Sokolov-Ternov polarizing mechanism however polarizes the beam along $\vec{B}$ which is now distinct from $\vec{n}_0(s)$ and looses its efficiency. The spin motion is highly perturbed, causing strong depolarization, when the spin precesses in phase with harmonics of the perturbations. The resonance condition for the strongest (linear) spin resonances is: $\nu = k + k_x Q_x + k_y Q_y + k_s Q_s$, with $|k_x| + |k_y| + |k_s| = 1$. The integer resonances concern the $\vec{n}_0(s)$ vector which is bent in the horizontal plane on resonance. The depolarization can be shown to be directly related to the square of the strength of the other linear spin resonances (betatron and essentially synchrotron). However, the calculation of the strength $J_{s,x,y}$ of these resonances in the small amplitude model shows that the strongest resonances for LEP depend on the tilt of the $\vec{n}_0(s)$ vector, i.e. on the integer resonances:

$$J_s \approx \oint K e^{i\psi}(D_y - D_x|\delta\vec{n}_0|e^{i\psi_0})ds \tag{12}$$

$$J_x \approx \oint |\delta\vec{n}_0|e^{i(\psi+\psi_0)}(K\sqrt{\beta_x}e^{\pm i\phi_x})ds \tag{13}$$

$$J_y \approx \oint e^{i\psi}(K\sqrt{\beta_y}e^{\pm i\phi_y})ds \tag{14}$$

ψ and ϕ are respectively the spin precession and betatron angles. K denotes the quadrupole strength and $D_{x,y}$ the horizontal and vertical dispersion. $\delta\vec{n}_0$ is the tilt of the precession axis. In LEP, the synchrotron resonance J_s is overwhelming [15, 2] and its term depending on the tilt of the precession axis dominates at small polarization levels. The Harmonic Spin Matching consists in minimizing the tilt of the spin precession axis to minimize the integrals expressing the strength of the depolarizing resonances. It can be further shown that the higher-order resonances which cannot be ignored in LEP are themselves proportional to the linear resonances and therefore are minimized as well. The method is called "harmonic" because it is done for a specific value of the spin tune. The resonance compensation relies on the calculation of a pattern of vertical orbit perturbations which reproduce the perturbation though with the opposite phase. HSM was anticipated by Baier and Orlov in 1966 [16]. It allowed to increase the polarization level from 40 to 80% in PETRA at 16.5 GeV [17, 18]. Its efficiency at the much higher energy of LEP was studied to establish the potential of LEP for polarization [19, 15]. It was successfully applied at TRISTAN [20] and HERA [21].

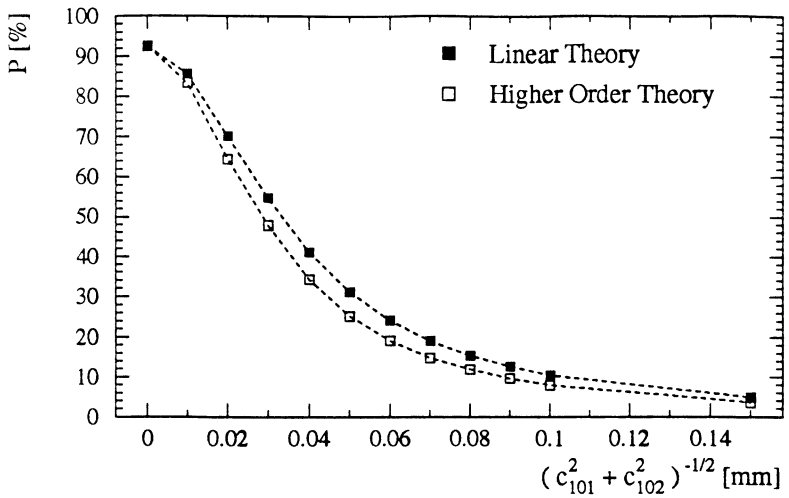

Figure 10: *Polarization versus strength of the two neighbouring harmonics of the vertical closed orbit. It is assumed that the spin tune is close to the half integer 101.5. The dependence has been calculated with linear and higher order theory from SODOM. From [5].*

4.2 Implementation

The tilt of the spin precession axis depends on the horizontal dipole fields along the closed orbit, i.e. mainly on the vertical beam position in the quadrupoles. Derbenev and Kondratenko showed that the contribution to the depolarization τ_p/τ_d by this tilt can be expressed in terms of the Fourier harmonics of the vertical closed orbit c_k [22]:

$$\frac{\tau_p}{\tau_d} \propto \nu^2 \sum_k \frac{|c_k|^2}{(\Delta\nu_k)^4} \tag{15}$$

The given formula is only valid in a linear approximation and assumes that synchroton oscillations of the particles dominate depolarization. The polarization is obtained from τ_p/τ_d through eq. 7. $\Delta\nu_k$ denotes the distance to the resonance k. If the spin tune ν is set close to the half-integer $k_0 + 0.5$ then only the two closest vertical orbit harmonics c_{k_0} and c_{k_0+1} contribute significantly to the depolarization. This characteristic was taken advantage of to predict the polarization level from the strengths of the two nearest resonances (fig. 10). This was used in practice to decide whether HSM is worth pursuing.

Because the rise-time of the polarization is much longer in LEP than in the other machines, a trial-and error compensation of the two near-by integer resonances would have taken at least 24 hours, i.e. would have been very difficult in practice. Therefore the possibility of doing HSM directly from the beam position information was investigated for LEP [5], taking into account the accuracy of the beam position monitors, their local alignment with respect to the near-by quadrupole and the overall alignment of the machine. It was shown that a tight re-alignment and the expected improvement of beam position measurements should yield a polarization of about 45% after deterministic HSM.

The procedure of deterministic HSM is now illustrated in more detail. Fig. 11 shows the measured vertical closed orbit after final standard orbit corrections. The integrated bending angle per cell is the periodic variable for the Fourier analysis of the closed orbit (selecting the frame where the spin precession is uniform). Therefore only the closed orbit in the arcs is important. The measured Fourier spectrum of the vertical closed orbit before HSM is shown in fig. 12 at the top. A pattern of 8 vertical closed orbit bumps is then calculated to compensate exactly one of the harmonics. The symmetry of the pattern is chosen such as not to perturb the

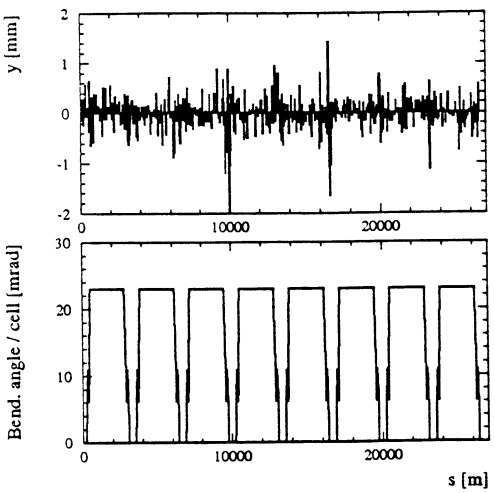

Figure 11: *Top: Measured vertical closed orbit before Harmonic Spin Matching. Bottom: The bending angle per cell is the periodic variable of the Fourier analysis.*

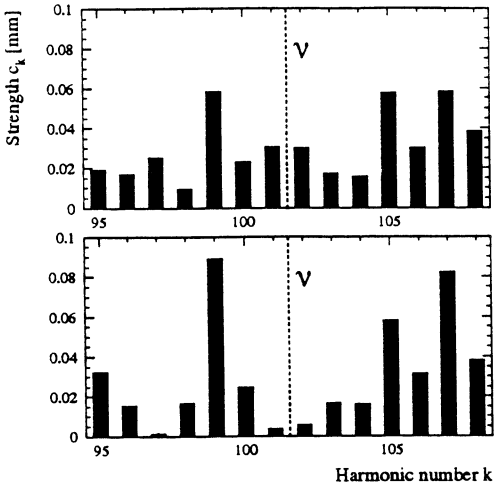

Figure 12: *Measured Fourier spectrum before (top) and after (bottom) Harmonic Spin Matching.*

three near-by harmonics. The spectrum of the corrected orbit is shown in fig. 12 at the bottom after sending the calculated orbit bumps for the two closest harmonics. The strengths of the harmonics 101 and 102 can be used to predict the expected polarization using fig. 10. Before HSM, the polarization is expected to be about 30% in higher order theory. Some lower value (20% - 25%) is a realistic estimate. The prediction refers indeed to a simplified yet reasonably realistic model (perfect orbit readings, no coupling,...). After application of the HSM bumps the harmonics were almost cancelled completely in the Fourier spectrum as can be seen in fig. 12. The expected polarization for the idealised case is now higher than 85% and there is no room for further deterministic improvement by this method.

4.3 Results

Already in the first polarization experiment in 1993 deterministic HSM was tried successfully and polarization could be increased from 8% to more than 30%. Its clear effect on polarization is in fig. 5 for a spin tune of 105.5 with the harmonics 105 and 106 compensated. Two other examples are shown in fig. 6 and in fig. 13 for a spin tune of 101.5 and the harmonics 101 and 102 compensated. Because the method was immediately found to increase significantly the asymptotic polarization level, there is limited information on the 'natural' polarization level before HSM in 1993. Fig. 14 shows all measured polarization degrees from the first measurement in 1990 up to now (excluding all energy calibration runs at end of physics coasts in 1993). The polarization measurements for 1993 are equally documented in appendix. Two conclusions can be drawn from fig. 14:

1. In 1993 the transverse polarization in LEP improved without HSM from a typical 10% to about 15% due to the quadrupole re-alignment and the better beam observation monitors (BOM). This improvement is less than expected but the statistics is very limited.

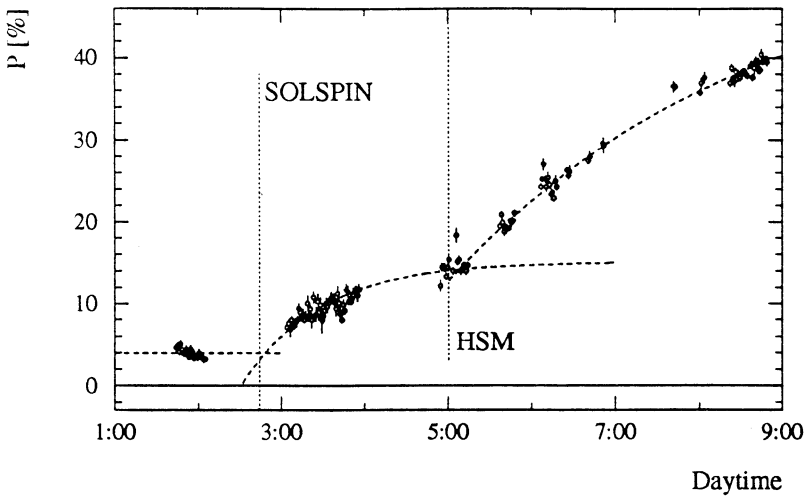

Figure 13: *Measured polarization as a function of time showing the effect of spin matching of the four experimental solenoids and the effect of deterministic Harmonic Spin Matching of the vertical closed orbit for a spin tune of 101.5.*

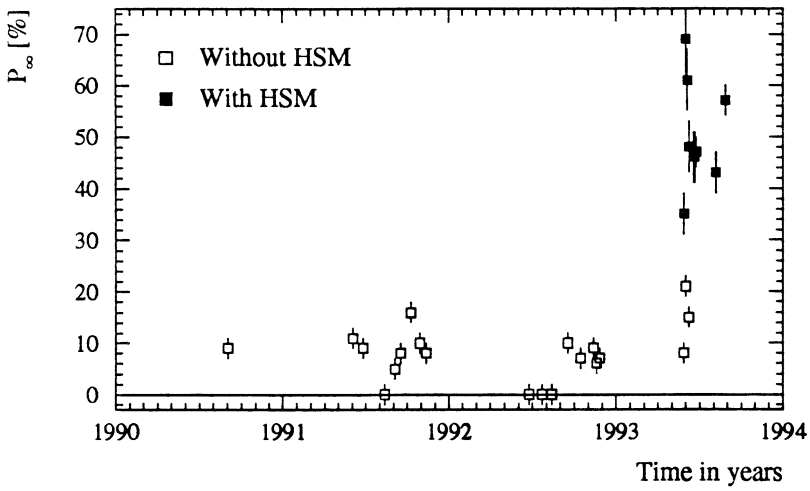

Figure 14: *Achieved equilibrium polarization degrees P_∞ are shown from the beginning of transverse polarization at LEP in 1990 up to now. Most polarization measurements from operational energy calibrations in 1993 are not included.*

2. With HSM, the asymptotic polarization increased to above 35% with an average of 50%. This shows that the accuracy of the knowledge of the orbit (including alignment) is better than expected.

On one occasion, it was tried to further improve the polarization by empirical HSM. This was done by changing the amplitudes of the applied harmonics in steps while observing the polarization level. The measured polarization reached 57% $\pm$ 3% at a spin tune of 101.5. The measurements are shown in fig. 15. Since they were performed in parallel to ongoing energy calibration it was not possible to tune the polarimeter on a regular basis and larger fluctuations in the signal than usually had to be accepted. However, during the time of maximum polarization the systematics of the measurements were well controlled. Close to the end of the experiment the rise time of polarization build-up was measured. Since the time of zero polarization and the equilibrium degree of polarization were known a precise calibration of the polarization scale could be done. The slow loss of polarization towards the end of the experiment was caused by uncorrected drifts of the closed orbit.

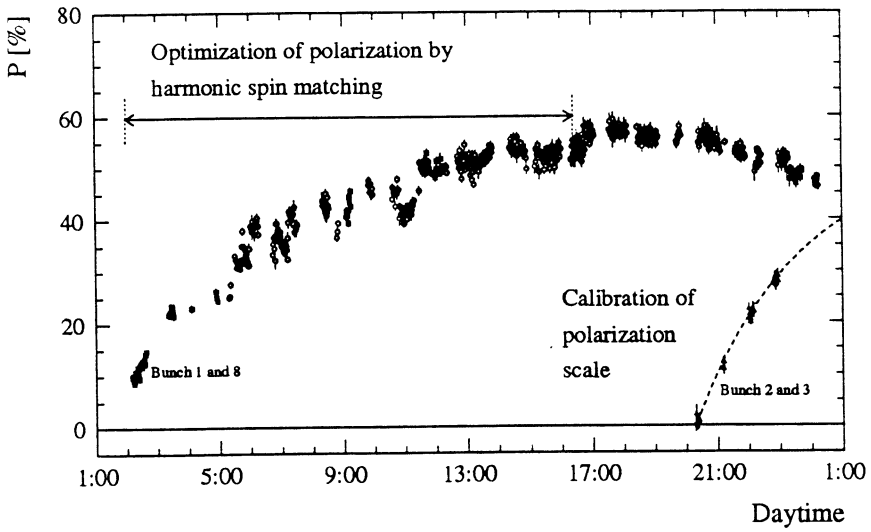

Figure 15: *The experiment with the maximum measured polarization of 57% ± 3% is shown. Polarization was optimized with deterministic and empirical Harmonic Spin Matching. At the end of the experiment the polarization scale was calibrated.*

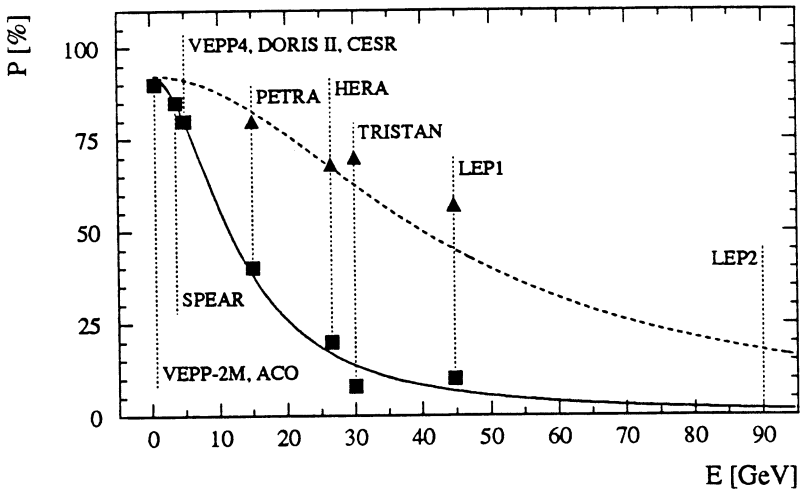

Figure 16: *Maximum measured polarization degrees are compared for different storage rings with Harmonic Spin Matching (triangles) and without Harmonic Spin Matching (squares). The measurements from SPEAR and HERA are extrapolated with beam energy using eq. 16. Equal imperfections for all machines and no depolarization from the beam energy spread are assumed.*

4.4 The scaling law for polarization

In fig. 16 the maximum observed polarization degrees are compared for different storage rings with and without HSM. The polarization degrees are taken from [23, 24, 20]. The polarization decreases as expected with the beam energy E. In the approximation of small amplitudes, assuming equal imperfections α for all storage rings the dependence of polarization on the beam energy can be written as [25]:

$$P = \frac{92.4\%}{1 + (\alpha E)^2} \tag{16}$$

The constant α was adjusted from SPEAR data (without HSM) and from HERA data (with HSM). This law shows that the small amplitude approximation is a valid model up to the LEP energy. If the higher-order spin resonances would have contributed to the depolarization, the dependence on the energy would be steeper with an exponent larger than 2. This does not mean that these resonances were not present, but that they could be avoided. Before LEP went into operation, strong depolarization by higher-order effects was indeed feared.

4.5 Limitation from vertical dispersion

Until now we only considered HSM of vertical closed orbit deviations, i.e. cancellation of the dominant term in the expression of the strength of the dominant depolarizing resonance (the synchrotron spin resonance, equation 12). The vertical dispersion arising from imperfections may cause depolarization too. It increases the vertical beam emittance and in this way enhances the vertical betatron spin resonances. These are however negligible at LEP. The Fourier spectrum of the dispersion enters into the excitation of the synchrotron spin resonances. It was shown by Montague that the influence from dispersion harmonics D_k extends much further than for orbit harmonics [26]:

$$\frac{\tau_p}{\tau_d} \propto \nu^2 \sum_k \frac{|D_k|^2}{(\Delta\nu_k)^2} \tag{17}$$

Furthermore, the higher-order satellite resonances are equally driven by dispersion.

The Fourier spectrum from a measurement of the vertical dispersion is shown in fig. 17. The RMS value of dispersion was 5.4 cm and during the experiment a polarization degree of 21% $\pm$ 2% was measured with a calculated asymptotic degree of 46% $\pm$ 5%. The spectrum in fig. 17 shows strong harmonics at spin tunes which fulfil the condition $Q_y \pm k \cdot 8$. k is any positive integer and Q_y is here understood as the integer part of the vertical betatron tune ($Q_y = 76$ for LEP in 1993). The appearance of systematic integer spin resonances is expected on these locations [11] and points out that the integer parts of the machine tunes and the beam energy must carefully be chosen in order to achieve high radiative polarization. For the case considered, the harmonics D_k around the spin tune 103 are small enough to be buried in the measurement noise (about 0.3 cm). Calculations show that, in presence of dispersion harmonics of this amplitude, the polarization is limited to 70%. No action was therefore undertaken to implement HSM of the vertical dispersion.

5 Higher-order spin resonances

Although higher-order spin resonances of the form $\nu = k \pm k_s Q_s$ with $k_s > 1$ have always been of concern, causing even depolarization when the small spin tune shift due to the terrestrial

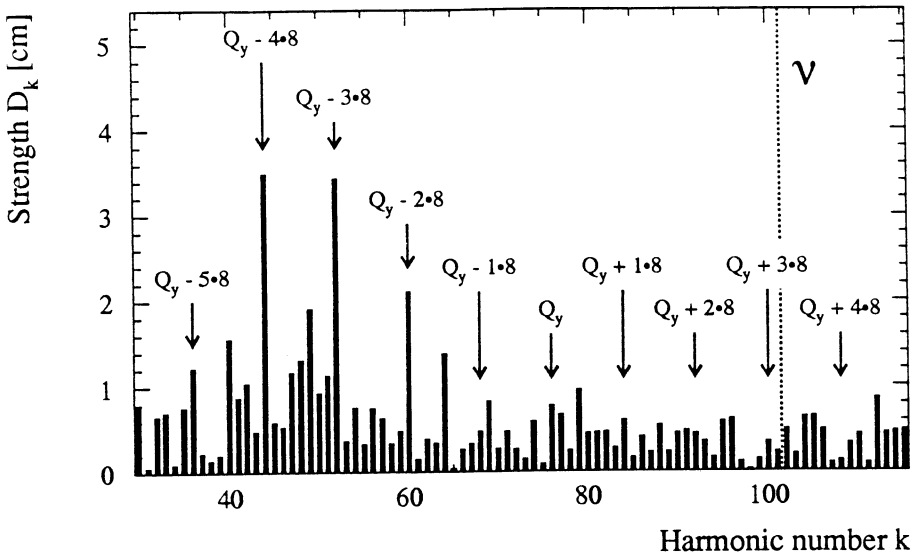

Figure 17: *The Fourier spectrum of the measured vertical dispersion in LEP. The locations of expected systematic integer spin resonances are marked.*

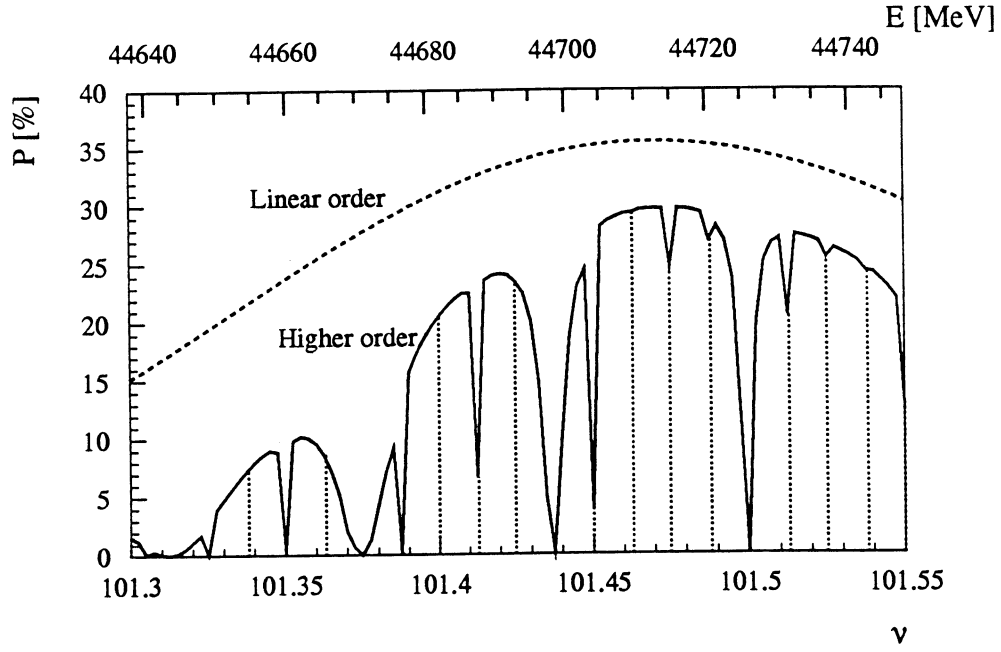

Figure 18: *Calculation of polarization including higher order spin resonances for a realistic LEP with polarization tunes. All possible resonances apart from those clearly showing up are marked by dotted lines. The resonance conditions can be looked up in table 1. The calculation was done with the SODOM module inside MAD [27, 31]. From [5].*

tides brought the spin tune in a resonance condition (they are spaced by 27 MeV only), we had previously not found the time to study them. In 1993, one of these resonances could be accurately measured and compared to the prediction of a new theory by Yokoya [27].

5.1 Higher-order calculations with SODOM

Because the polarization depends on the details of the optics and the imperfections, it can only be calculated by computer programs. For studies and experiments, the program SITF [28, 29] is used. It calculates the polarization in the small amplitude approximation and is sufficient for most purposes. The calculation of the higher-order effects in LEP has been a difficulty because the perturbative approach would not converge, given the not small amplitude of the synchrotron oscillation. For this reason, the evaluation of the importance of the higher-order effects had been carried out by a Monte-Carlo method [30, 15]. A new non-perturbative approach (SODOM) by Yokoya became recently available and implemented in MAD [31]. Because of the complexity of the calculations, the use of SODOM is limited by the available computer resources. It is nevertheless possible to compute the synchrotron satellites of the linear spin resonances which had been shown to dominate other higher-order effect at LEP [15].

Linear and higher-order polarization calculations are shown in fig. 18 for a realistic LEP model with about 30% maximum polarization [5]. The resonance conditions, marked with dotted lines in fig. 18, can be looked up in table 1. In the experimental conditions, it appears that the synchrotron satellites of the integer resonances are strong and clearly visible at 101.3125, 101.375, 101.4375 and 101.5. They decrease somewhat the asymptotic level of polarization between resonances. The other higher order spin resonances are weak and their width is smaller than the binning of the calculation. Due to the restricted knowledge of the "real" LEP their strengths cannot be predicted in detail.

5.2 Measurements of higher-order spin resonances

In order to measure higher-order spin resonances, the polarization must be observed as a function of spin tune. For LEP this is a very delicate experiment since the build-up time for polarization is long. The spin tune (proportional to the energy) of the circulating beams is varied by changing the RF-frequency f_{RF}. The smallest possible change in f_{RF} is 2 Hz which is equivalent to a change of .00310 in spin tune or 1.37 MeV in beam energy (with the spin tune at 101.5 and a momentum compaction factor $\alpha = 1.86 \cdot 10^{-4}$). From fig. 18 it was decided that the sixth-order synchrotron satellite of 101 at 101.375 is sufficiently broad to be measurable in detail with the available resolution in beam energy.

To get close to the selected synchrotron satellite the spin tune was stepped from its initial value of 101.468 to 101.457, 101.417, 101.405, 101.393 and 101.357. For each spin tune the energy was measured by resonant depolarization. As expected the polarization degraded slowly when going down in energy and no unexpected higher-order spin resonance with sharp depolarization showed up. By following this procedure the momentum compaction factor α for LEP could precisely be measured to be $\alpha = (1.860 \pm 0.020) \cdot 10^{-4}$. This is in excellent agreement with the calculated value for LEP which is $\alpha = 1.859 \cdot 10^{-4}$.

The expected center of the $101+6 \cdot Q_s$ resonance was approached by jumping symmetrically from one side of the resonance to the other and measuring each point for at least 10 minutes. This strategy allowed to measure the full resonance and not only half of it. The measurement was completed in a short time (2:30 hours) and in one go. This is important to avoid uncontrolled shifts. The tidal effect was corrected for. The resulting measurements are shown on

Spin Tune	Resonance Condition	Spin Tune	Resonance Condition
101.3125	$101 + 5\cdot Q_s$ $102 - 11\cdot Q_s$	101.4375	$101 + 7\cdot Q_s$ $102 - 9\cdot Q_s$
101.3250	$101 + Q_y + 2\cdot Q_s$ $102 + Q_y - 14\cdot Q_s$ $102 - Q_x - Q_y - 6\cdot Q_s$	101.4500	$101 + Q_y + 4\cdot Q_s$ $102 + Q_y - 12\cdot Q_s$ $102 - Q_x - Q_y - 4\cdot Q_s$
101.3375	$101 - Q_x + 7\cdot Q_s$ $101 + Q_x - Q_y + 7\cdot Q_s$ $102 - Q_x - 9\cdot Q_s$ $102 + Q_x - Q_y - 9\cdot Q_s$	101.4625	$101 - Q_x + 9\cdot Q_s$ $101 + Q_x - Q_y + 9\cdot Q_s$ $102 - Q_x - 7\cdot Q_s$ $102 + Q_x - Q_y - 7\cdot Q_s$
101.3500	$101 + Q_x + 4\cdot Q_s$ $101 - Q_x + Q_y + 4\cdot Q_s$ $102 + Q_x - 12\cdot Q_s$ $102 - Q_x + Q_y - 12\cdot Q_s$	101.4750	$101 + Q_x + 6\cdot Q_s$ $101 - Q_x + Q_y + 6\cdot Q_s$ $102 + Q_x - 10\cdot Q_s$ $102 - Q_x + Q_y - 10\cdot Q_s$
101.3625	$101 - Q_y + 9\cdot Q_s$ $102 - Q_y - 7\cdot Q_s$ $101 + Q_x + Q_y + Q_s$	101.4875	$101 - Q_y + 11\cdot Q_s$ $102 - Q_y - 5\cdot Q_s$ $101 + Q_x + Q_y + 3\cdot Q_s$
101.3750	$101 + 6\cdot Q_s$ $102 - 10\cdot Q_s$	101.5000	$101 + 8\cdot Q_s$ $102 - 8\cdot Q_s$
101.3875	$101 + Q_y + 3\cdot Q_s$ $102 + Q_y - 13\cdot Q_s$ $102 - Q_x - Q_y - 5\cdot Q_s$	101.5125	$101 + Q_y + 5\cdot Q_s$ $102 + Q_y - 11\cdot Q_s$ $102 - Q_x - Q_y - 3\cdot Q_s$
101.4000	$101 - Q_x + 8\cdot Q_s$ $101 + Q_x - Q_y + 8\cdot Q_s$ $102 - Q_x - 8\cdot Q_s$ $102 + Q_x - Q_y - 8\cdot Q_s$	101.5250	$101 - Q_x + 10\cdot Q_s$ $101 + Q_x - Q_y + 10\cdot Q_s$ $102 - Q_x - 6\cdot Q_s$ $102 + Q_x - Q_y - 6\cdot Q_s$
101.4125	$101 + Q_x + 5\cdot Q_s$ $101 - Q_x + Q_y + 5\cdot Q_s$ $102 + Q_x - 11\cdot Q_s$ $102 - Q_x + Q_y - 11\cdot Q_s$	101.5375	$101 + Q_x + 7\cdot Q_s$ $101 - Q_x + Q_y + 7\cdot Q_s$ $102 + Q_x - 9\cdot Q_s$ $102 - Q_x + Q_y - 9\cdot Q_s$
101.4250	$101 - Q_y + 10\cdot Q_s$ $102 - Q_y - 6\cdot Q_s$ $101 + Q_x + Q_y + 2\cdot Q_s$	101.5500	$101 - Q_y + 12\cdot Q_s$ $102 - Q_y - 4\cdot Q_s$ $101 + Q_x + Q_y + 4\cdot Q_s$

Table 1: *Spin resonances from fig. 18 with polarization tunes (Q_x=90.10, Q_y=76.20, Q_s=0.0625) and for order 1 in Q_x and Q_y. The spin tunes between these resonances are safe for polarization. Higher order resonances in Q_x and Q_y which would appear at the same locations are given as well.*

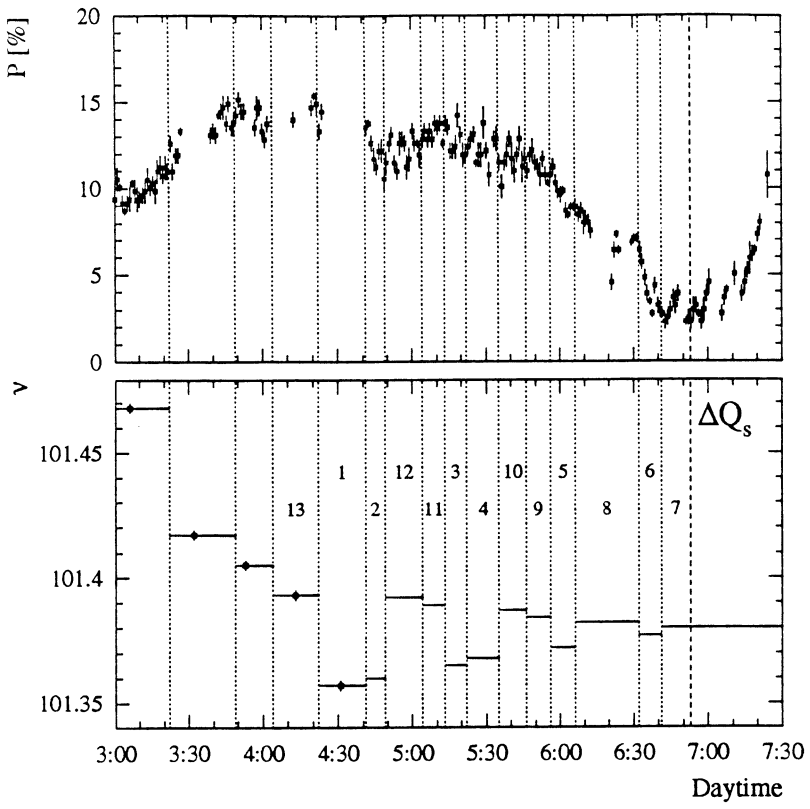

Figure 19: *Polarization as a function of time (top) for different beam energies (bottom). On the bottom the measured beam energies are indicated by points. The lines give the piecewise constant extrapolation taking the RF-frequency and tidal deformations into account. The numbers refer to the points in fig. 20 when counting from left to right. It is seen that polarization clearly degraded when the expected 6·Q_s resonance was approached. After changing Q_s the polarization signal recovered.*

fig. 19. It can be seen that the fast measurement had the disadvantage that often the equilibrium degree of polarization could not be measured. The "depolarization strength" τ_p/τ_d and the equilibrium degree of polarization P_∞ is therefore calculated from the measured slope P' of polarization at a time with initial polarization P_i:

$$\frac{\tau_p}{\tau_d} = \frac{92.4\%}{P_i} - \frac{P'\tau_p}{P_i} - 1. \tag{18}$$

This formula can be derived from eq. 7 and expresses the fact that for a given P_∞ the slope of polarization build-up at each intermediate polarization value P_i is fixed. The slope of polarization is determined from the measured data with a simple fit. The asymptotic polarization P_∞ is then calculated from:

$$P_\infty = \frac{92.4\%}{1 + \frac{\tau_p}{\tau_d}} \quad . \tag{19}$$

The "depolarization strength" τ_p/τ_d, obtained by this method, versus spin tune is shown in fig. 20. Two spin resonances show up. The narrow resonance has been detected only with the measured slope whilst the broad resonance was also measured explicitly with very small equilibrium polarization degrees. The spin resonances were fitted with the theoretically expected shape [32]:

$$\frac{\tau_p}{\tau_d} = \frac{\varepsilon}{(\nu - \nu_0)^2} + \left(\frac{\tau_p}{\tau_d}\right)_0, \tag{20}$$

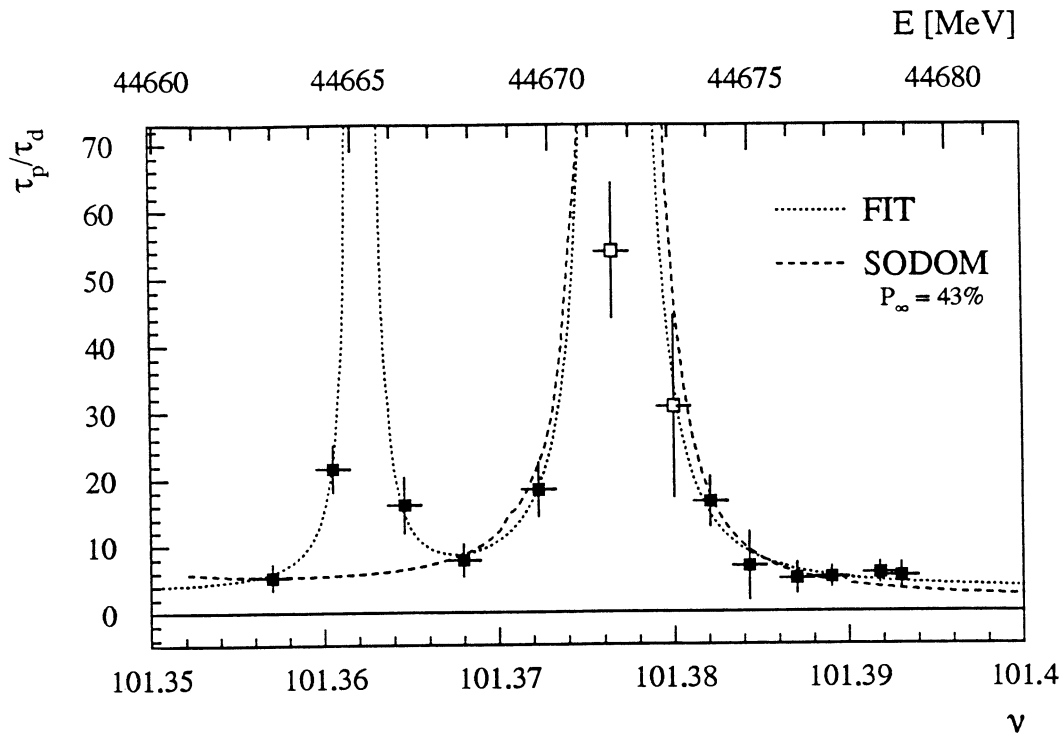

Figure 20: *The measured depolarization τ_p/τ_d versus spin tune shows two higher-order resonances. The expected theoretical resonant shape was fitted to the filled points. The open points were measured with a small degree of polarization and are therefore affected by systematic errors due to small polarization offsets. Even for small offsets (here we assume $\Delta P = 1.1\%$) they get large errors. As the open points are close to the center of the spin resonance where depolarization becomes infinity and as it is impossible to measure infinity they are excluded from the fit. The measured data and the fitted resonance shape are compared to the prediction from SODOM for a disturbed LEP model with an equilibrium polarization of about 43%. The SODOM calculations include only the $101 + 6 \cdot Q_s$ resonance and are shifted by $\Delta\nu = 0.0021$.*

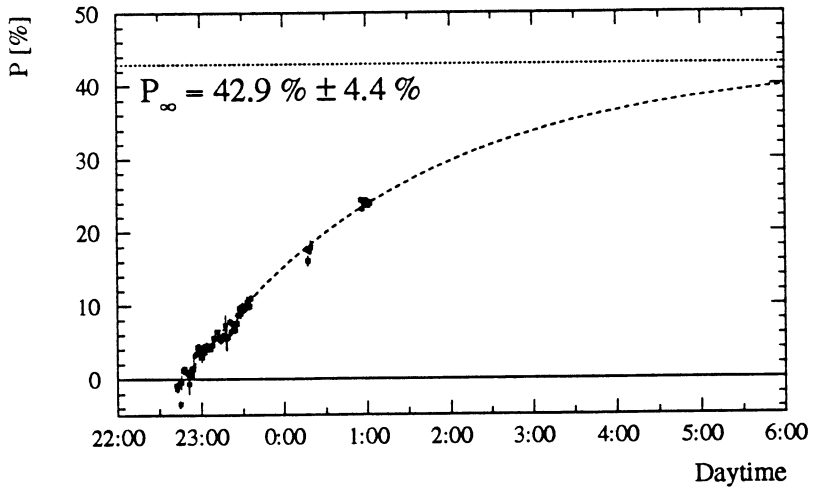

Figure 21: *Fit of the polarization build-up for the experiment from fig. 20. As the polarization scale is known a simple 2-parameter fit can be performed. Free parameters are the effective build-up time and the time of zero polarization. The equilibrium polarization is then obtained with good accuracy.*

$\varepsilon/10^{-4}$	ν_0	ν_{exp}	$\nu_0 - \nu_{exp}$	$(\tau_p/\tau_d)_0$
3.35 ± 0.71	101.3771 ± 0.0005	101.3750 ± 0.0012	0.0021 ± 0.0013	3.77 ± 1.03
0.57 ± 0.15	101.3623 ± 0.0003	-	-	3.77 ± 1.03

Table 2: *Results of a combined fit to the higher order spin resonances from fig. 20. The fitted central spin tune ν_0 for the broader resonance is compared with the expected spin tune ν_{exp} assuming that the observed resonance is the $101+6\cdot Q_s$ resonance. The accuracy in the measurement of the coherent synchroton tune is assumed to be $\Delta Q_s = .0002$.*

where ε is the strength of the resonance, ν_0 is the central spin tune and $(\tau_p/\tau_d)_0$ is the depolarization from other resonances which is assumed to be constant over the considered range. The results from a combined fit are given in table 2.

The equilibrium polarization close to the half-integer was calculated from the measured build-up of polarization (Fig. 21) and was used to adjust the LEP imperfections in the model so as to obtain the same asymptotic polarization. SODOM was then used to predict the width of the $101 + 6Q_s$ spin resonance which is found to be in good agreement with the measured width (see fig. 20). This measurement shows the important role of synchrotron satellites of the integer resonances for polarization at LEP and confirms the predictions from theoretical calculations remarkably well.

From table 2 the difference between the expected and the measured location of the $101 + 6Q_s$ spin resonance is found to be .0021 in spin tune (or 0.9 MeV in energy). However, the interpretation of this difference is delicate since the expected spin tune ν_{exp} was calculated with the coherent synchroton tune Q_s^{coh}. The coherent detuning is not precisely known at 46 GeV. Since the incoherent tune is larger than the coherent one the location of the spin resonance would appear shifted upwards against the location expected from Q_s^{coh}. If we assume that the energy scale is perfectly right the observed difference can be explained by a 0.6% larger incoherent synchroton tune.

The spin tune scale could possibly be shifted by interference effects. The expected bias would shift the spin tune scale and the measured location of the spin resonance downwards. This effect has the opposite sign compared to the detuning effect. Therefore we must interpret the observed difference between measured and expected location of the $101+6Q_s$ spin resonance as the remainder after compensation of the two effects. The upper bound for detuning of the synchroton tune in LEP is estimated to be 7%. From this we can conclude that the possible bias in the spin tune scale is smaller than 11 MeV. From other experiments we actually know that the bias is much smaller than this.

As already mentioned a narrow spin resonance shows up in fig. 21. We consider the hypothesis that it is the $102 - 10Q_s$ spin resonance. However, its measured width is about a factor of 4 larger than expected. We assume that this can be contributed to uncertainties in the measurements. Then the distance between the two measured resonances is $16 \cdot \Delta Q_s$ with ΔQ_s being the effect from detuning. We then arrive at a coherent detuning $\Delta Q_s/0.0625$ of about 1.5%. In this hypothesis the spin tune scale follows to be shifted by -1.5 MeV. The sign and the size of this bias is consistent with the expectations. Since it is not proven that the narrow spin resonance is in fact the $102 - 10Q_s$ resonance the result should be interpreted with care.

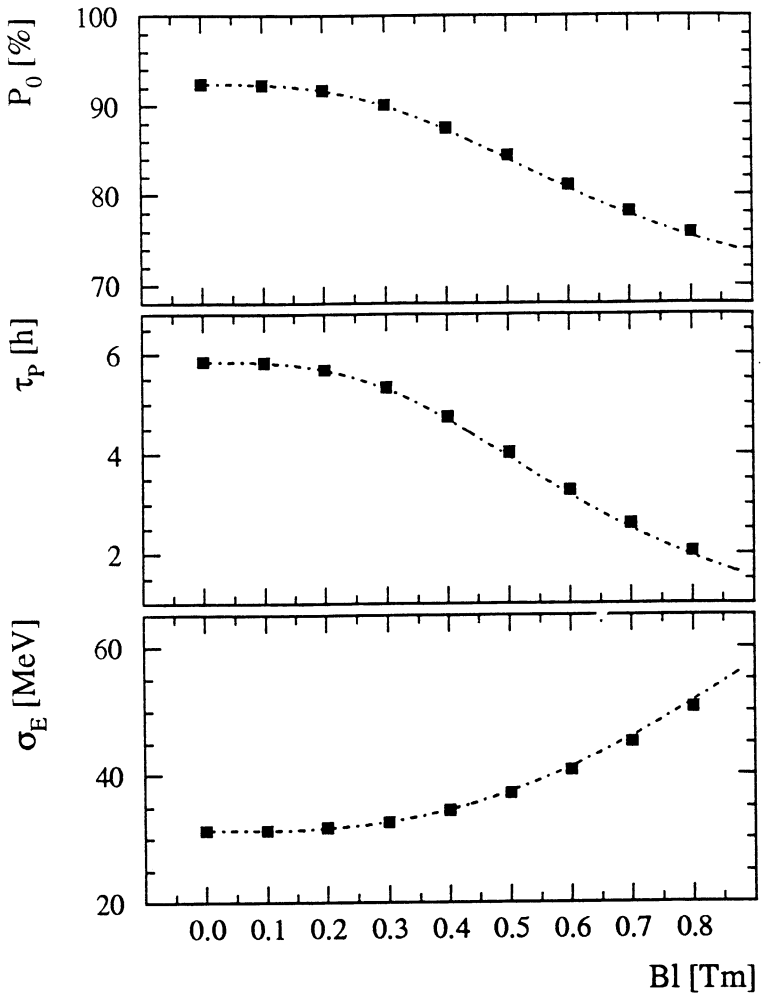

Figure 22: *Natural Sokolov-Ternov polarization degree P_0, natural polarization build-up time τ_p and beam energy spread σ_E versus integrated field B per damping wiggler. All damping wigglers are at the same field and the spin tune is assumed to be at 101.5. The results from SODOM (squares) are compared to the analytical calculation (curve). From [5].*

6 Speeding up the polarization rise with asymmetric wigglers

The natural time constant τ_p for the radiative build-up of transverse beam polarization at LEP1 to its maximum degree of 92.4% is between 5 and 6 hours. τ_p is reduced to some effective build-up time τ_p^{eff} by the depolarization process, e.g. to about 30 minutes for 10% polarization. However, high polarization can only be observed after a time of the order of many hours which is long for practical purposes.

Asymmetric wigglers can reduce τ_p substantially. The experiments carried out were done with the damping wigglers which are fully operational. They are asymmetric and reduce τ_p by a factor 2.9 when each wiggler is set to its maximum integrated field of 0.8 Tm. The damping wigglers are located at small dispersion values; their influence on the beam emittances is small.

Wigglers do not only shorten the build-up time of polarization but at the same time decrease the natural Sokolov-Ternov polarization level and more seriously increase the energy spread of the particle beam. The three effects are shown in fig. 22 as a function of the integrated field per wiggler. All four damping wigglers are assumed to be at the same field. The results on beam characteristics and linear polarization agree very well for SITF, SODOM and for available analytical calculations [33].

6.1 Depolarization due to energy spread

The absolute beam energy spread σ_E scales with the square of the beam energy E while the spin resonance spacing remains constant. It has long been expected from analytical calculations that at some stage the polarization would be limited by the beam energy spread [34, 35]. However, numerical higher-order calculations with the Monte-carlo code SITROS predicted high polarization for LEP1 with wigglers [15]. The energy spread in the considered case was 78 MeV which is roughly twice the LEP1 energy spread.

The principle of the depolarization enhancement due to energy spread is illustrated in fig. 23. The spin tune domain where polarization can develop is only a fraction of the integer resonance spacing (440 MeV). As the beam energy spread is increased by the wigglers or the increased beam energy, it becomes impossible to avoid strong linear resonances. The polarization calculation in fig. 23 indicates that already at LEP1 the polarization is slightly affected by the depolarization due to energy spread.

Using the damping wigglers the beam energy spread can be increased in a smooth way. On several occasions the damping wigglers were switched on and the polarization was measured. The most complete example is shown in fig. 24 where the measured polarization is shown for different settings of the damping wigglers. The spin tune during this experiment was very carefully kept between higher order spin resonances. It is clearly seen that polarization decreased substantially when the damping wigglers were ramped up. The interpretation of the results from fig. 24 is not straightforward since for most of the wiggler settings the equilibrium degree of polarization was not measured (there was not enough time to wait for it). As shown earlier the equilibrium polarization P_∞ can, however, be calculated from the measured slope P' of polarization at some time with initial polarization P_i. The formula for the case without wigglers was given in eq. 18. Taking into account the effects from wigglers the natural build-up time τ_p must be replaced by its reduced value τ_p^W and the natural polarization $P_0 = 92.4\%$ must be replaced by its reduced value P_0^W.

Analysing the data with the slope P' for each setting of the damping wigglers yields the dependence of the equilibrium polarization on the integrated magnetic field in each damping wiggler. The result is shown in fig. 25. Experimental results from other experiments are added in the figure. The measurements agree well with each other and show a strong loss of polarization with increasing fields in the damping wigglers. The equilibrium polarization is reduced to less than 8% with the damping wigglers at full field.

The measurements are compared to the calculated polarization in linear and higher-order theory. In order to exclude possible effects from the beam emittances in the calculations, a perfect LEP model was only perturbed locally by HSM bumps. In this way, the polarization level can be adjusted to the measured value without exciting a vertical dispersion: the horizontal dispersion was smaller than 1 cm and the vertical dispersion was smaller than 0.5 cm at the locations of the damping wigglers. The polarization for this LEP model with the damping wigglers at minimum field is about 50%. The linear calculation shows a slight decrease of polarization with increasing wiggler field. This is due to the decrease in the natural Sokolov-Ternov polarization degree P_0 from fig. 22. However, the higher-order calculation shows a strong loss of polarization, comparable to the one observed in the measurements, which was not observed in the Monte-carlo studies.

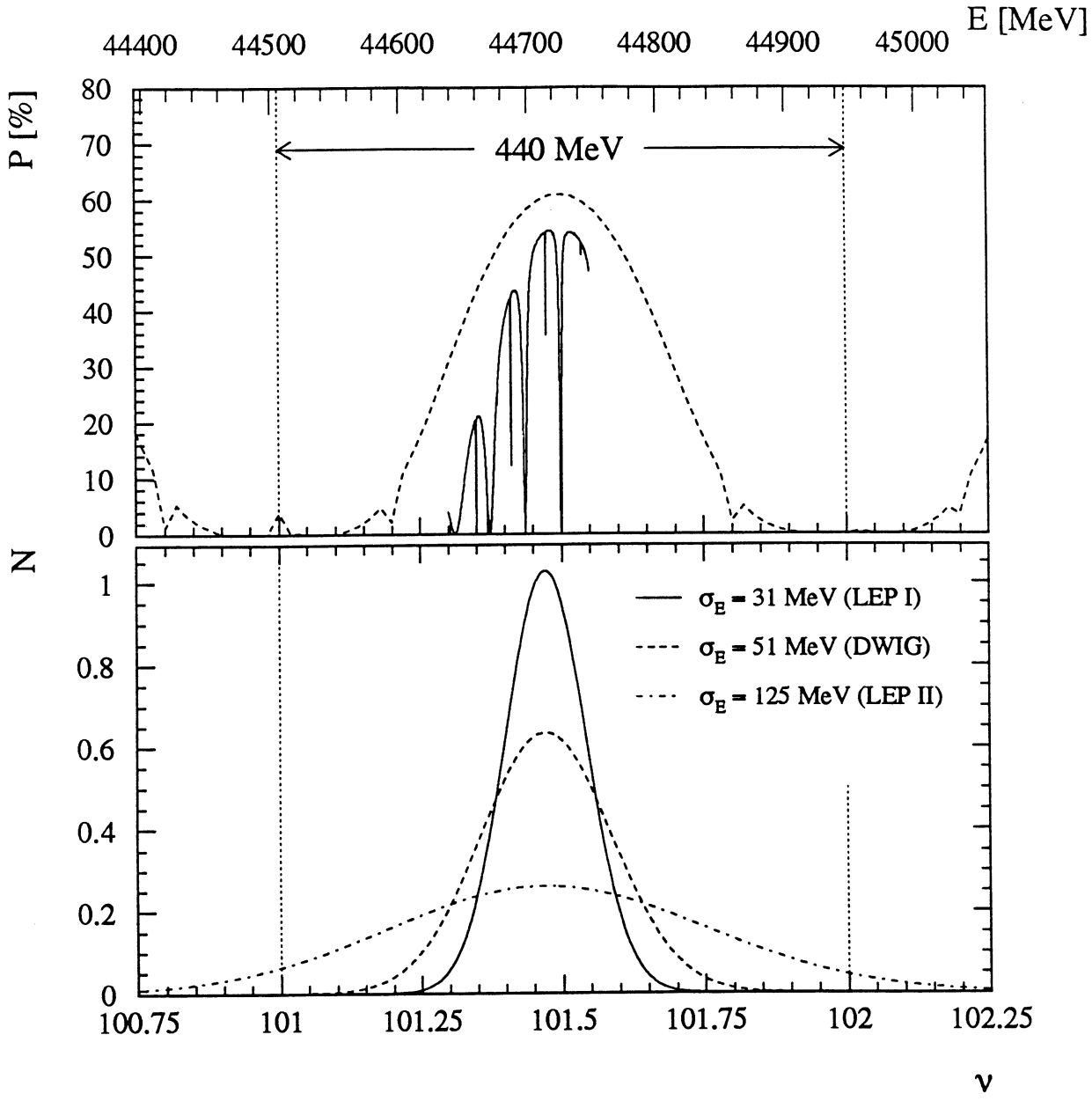

Figure 23: *Top: The spacing of linear spin resonances is illustrated from polarization calculations for LEP1 without wigglers. The linear case is compared to the higher-order case. Bottom: The energy distribution of particles in a Gaussian beam is shown for three cases: LEP1, LEP2 and LEP1 with damping wigglers on maximum field (DWIG). The spin tune is assumed to be at 101.47. From [5].*

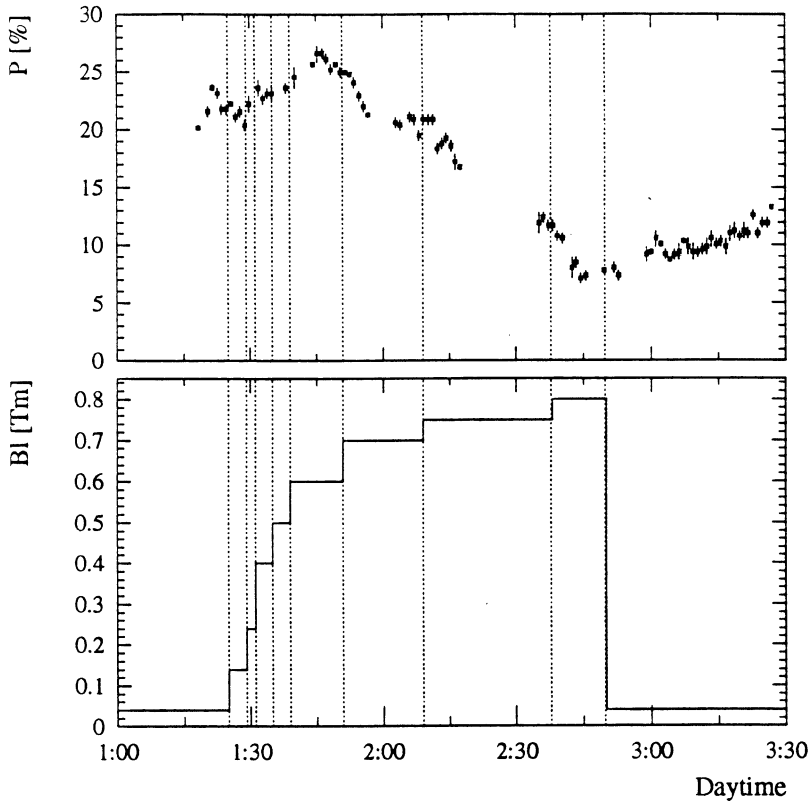

Figure 24: *Measured polarization for different settings of the integrated B-field at all damping wigglers. The minimum field is 0.04 Tm.*

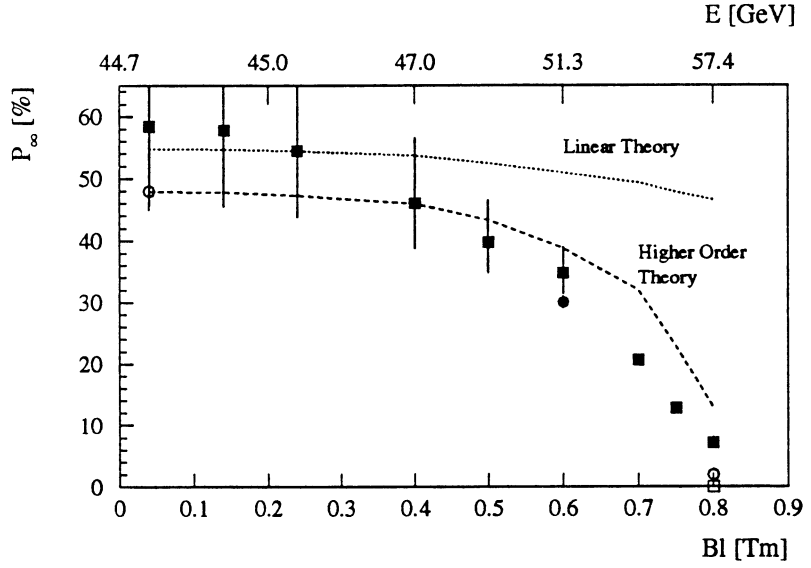

Figure 25: *Equilibrium polarization P_∞ as a function of the integrated magnetic field B at all damping wigglers. The different symbols indicate results from different experiments. The measurements are compared to calculations in linear and higher-order theory. The upper horizontal scale gives the beam energy needed to get the same energy spread as from the wigglers.*

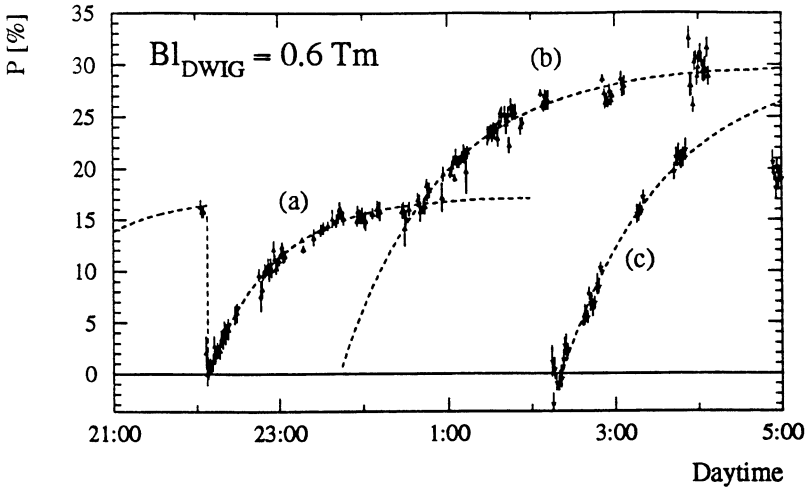

Figure 26: *Three measured polarization build-up curves with the damping wigglers at 0.6 Tm each. Up to 30% polarization was achieved after a second step of deterministic Harmonic Spin Matching.*

Case	τ_p^W [h]	τ_p/τ_p^W
(a)	3.82 ± 0.34	1.53 ± 0.14
(b)	3.23 ± 0.31	1.81 ± 0.17
(c)	3.35 ± 0.21	1.75 ± 0.11

Table 3: *Reduced build-up time τ_p^W for the damping wigglers at 0.6 Tm each. The results are obtained from three different fits to the results shown in fig. 26 (case (a), (b) and (c)). The ratio τ_p/τ_p^W is also given and should be compared to the expected value of 1.8.*

6.2 Reduction of polarization build-up time

From the results in the previous section it is seen that polarization can be found with the damping wigglers at 0.6 Tm each. The polarization build-up time τ_p is approximately halved for this field. An experiment was performed with the damping wigglers at 0.6 Tm. The polarization build-up was measured three times on different bunches and the result is shown in fig. 26. An equilibrium polarization of 30% was achieved in good agreement with the expectation. A decrease in the natural polarization build-up time τ_p by a factor 1.8 was expected. The rise-time of the polarization with wigglers may be computed from the fitted effective rise-time and the measured asymptotic polarization.

$$\tau_p^W = \frac{\tau_p^{\mathrm{eff},W} \cdot P_0^W}{\Delta y_\infty^W} \cdot \xi \quad . \tag{21}$$

The resulting τ_p^W's for fig. 26 are given in table 3 where also the factor of reduction in τ_p is calculated. An offset error on the center-of-gravity-shift of 5μm was assumed. The results are compatible with the expected decrease in τ_p by a factor of 1.8. Especially the two fits with an asymptotic polarization of 30% (case (b) and (c)) confirm very well the expectation. Within the errors all results are in agreement with the expectation and we conclude that the polarization build-up time for LEP was successfully reduced with asymmetric wigglers.

7 Conclusions

The efforts invested to facilitate the energy calibration by resonant depolarization (optics change, tight re-alignment, upgrade of the beam observation system) were rewarded even somewhat beyond the expectations. The high accuracy of the beam observation system allowed to compute directly from the measured orbit the tilt of the spin precession axis which could then be corrected by Harmonic Spin Matching. Polarized beams could be obtained routinely for experiments and physics at three energies. Measured polarizations up to 57% $\pm$ 3% were obtained with four compensated experimental solenoids. Globally, the results of the experiments show that the predictive power of the theory of polarization in the small amplitude approximation is still remarkable at the LEP energy of 45 GeV. Higher-order effects are there nevertheless; the width of the numerous additional resonances is still sufficiently narrow to allow the simpler model to hold between them. However their enhancement due to an increase of the beam energy spread by the wigglers causes rapidly strong depolarization. The detailed calculation of these higher-order effects had not been very successful in the past. The new approach by Yokoya seems in good quantitative agreement with the measured higher-order resonance and the measured variation of the polarization versus beam energy spread. If this agreement is further confirmed experimentally, polarization at LEP 2 will not be possible, as foreseen by analytical calculations and possibly in contradiction with former Monte-Carlo calculations. However, the beams would be polarized at all energies in a perfect accelerator. The ultimate energy at which polarization will be obtained will thus depend on practical limits on accuracy, stability .... The improved understanding allows now to be confident that the spin can be efficiently rotated into the longitudinal plane at 46 GeV. The influence of the beam-beam effect on the polarization remains to be studied.

Acknowledgements

We would like to thank the LEP Operations group for his help, K. Yokoya for providing us with his SODOM program and Yu. Eidelman for helpful discussions. Further we thank all the people who worked on improvements of the polarimeter, the alignment and the BOM system of LEP. We thank CERN, the Max-Planck-Institut für Physik, München, and the Ecole Polytechnique, Paris, for their support.

References

[1] R. Assmann, J.P. Koutchouk, A. Verdier. Contributions to the 3rd Workshop on LEP Performance. In J. Poole (Ed.), "Proceedings of the Third Workshop on LEP Performance", Chamonix, January, 10-16 1993, CERN SL/93-19(DI) (1993).

[2] R. Assmann: "Results of Polarization and Optimisation Simulations". In J. Poole (Ed.), "Proceedings of the Third Workshop on LEP Performance", Chamonix, January, 10-16 1993, CERN SL/93-19(DI) (1993) 341.

[3] G. Alexander et al.: "Measurements of Polarization in LEP". In: "Polarization at LEP", G. Alexander et al., eds., CERN Yellow report 88-06 (1988) Vol.II, 3.

[4] M. Placidi and R. Rossmanith: "e^+e^- Polarimetry at LEP". Nucl. Instr. and Meth. A274(1989)79.

[5] R. Assmann: "Transversale Spin-Polarisation und ihre Anwendung für Präzisionsmessungen bei LEP". PhD thesis at the Ludwigs-Maximilians-Universität München, 1994. To be published.

[6] B. Dehning: "Performance of the LEP polarimeter". In J. Poole (Ed.), "Proceedings of the Third Workshop on LEP Performance", Chamonix, January 10-16, 1993, CERN SL/93-19(DI) (1993) 239.

[7] R. Schmidt et al.: "Performance and Limitations of the LEP Polarimeter". Proc. 35^{th} Yamada Conference, 10^{th} International Symposium on High Energy Spin Physics, Nagoya, Japan, 9-14. Nov. 1992.

[8] M. Placidi (Polarization Collaboration): "Polarization Results and Future Perspectives". In J. Poole (Ed.), "Proceedings of the Third Workshop on LEP Performance", Chamonix, January 10-16, 1993, CERN SL/93-19(DI) (1993) 281.

[9] A. Blondel: "Compensation of Integer Spin Resonances Created by Experimental Solenoids". LEP Note 629 (1990).

[10] R. Bailey et al.: "Comissioning and Operation of the LEP Pretzel Scheme". Proc. of the 1993 IEEE Part. Acc. Conf., Washington D.C., May 17-20, 1993.

[11] J.P. Koutchouk: "Systematic Integer Spin Resonances". CERN LEP-TH/88-47.

[12] J.P. Koutchouk et al.: "Energy Calibration with a Polarized Beam at LEP". Proc. 16^{th} Intern. Conf. High Energy Acc., Hamburg, Germany, 1992.

[13] L. Arnaudon et al.: "Energy Calibration of LEP in 1993 with Resonant Depolarization". To be published.

[14] J. Buon and J.P. Koutchouk: "Polarization of Electron and Proton beams". CERN advanced accelerator school, Rhodos, 1993, to be published.

[15] J.P. Koutchouk and T. Limberg: "Polarization Simulation Studies for LEP". In: "Polarization at LEP", G. Alexander et al., eds., CERN Yellow report 88-06 (1988) Vol.II, 204.

[16] V.N. Baier and Yu.F. Orlov: "Quantum Depolarization of Electrons in a Magnetic Field". Sov. Phys. Dokl. 10(1966)1145.

[17] H.D. Bremer, DESY 82-026.

[18] R. Rossmanith and R. Schmidt: "Compensation of Depolarizing Effects in Electron Positron Storage Rings". Nucl. Instr. Meth. Phys. Res., A236(1985)231.

[19] J.P. Koutchouk : "Polarization simulation results for LEP". Proceedings of the Workshop on Polarization in LEP, CERN, Geneva, 1987.

[20] K. Nakajima: "Polarization Study in TRISTAN". Proc. of the 3^{rd} European Particle Accelerator Conf., Berlin, March 1992. H. Henke et al. (eds), Edition Frontieres 1993.

[21] D.P. Barber et al.: "High Spin Polarisation at the HERA Electron Storage Ring". DESY 93-038.

[22] Ya.S. Derbenev, A.M. Kontratenko and A.N. Skrinsky: "Radiative Polarization at Ultra-High Energergies.". Part. Acc. 9(1979)247.

[23] Yu.M. Shatunov: "Polarized Beams of High Energy Electrons and Positrons". Part. Acc. 32(1990)139.

[24] D.P. Barber. Private communication.

[25] A.W. Chao: "Latest on Polarization in Electron Storage Rings". SLAC-PUB-3081 (1983).

[26] B.W. Montague: "Polarized Beams in High Energy Storage Rings". Physics Reports (Rev. section of Phys. Lett.) 113, No. 1(1984)1.

[27] K. Yokoya: "Non-perturbative Calculation of Equilibrium Polarization of Stored Electron Beams". KEK Report 92-6 (1992).

[28] A.W. Chao: "Evaluation of Radiative Spin Polarization in an Electron Storage Ring". Nucl. Instr. Meth. 180(1981)29-36.

[29] A. Ackermann, J. Kewisch and T. Limberg. Implemented into MAD be H. Grote. To be published.

[30] J. Kewisch, DESY 83-032 (1983).

[31] H. Grote: "MAD-SODOM User's Guide". CERN-SL/93-40 (AP).

[32] J. Buon: "A Stochastic Model of Depolarization Enhancement due to Large Energy Spread in Electron Storage Rings".

[33] A. Blondel and J.M. Jowett: "Wigglers for Polarization". In: "Polarization at LEP", G. Alexander et al., eds., CERN Yellow report 88-06 (1988) Vol.II, 216.

[34] C. Biscari, J. Buon and B.W. Montague: "Depolarizing Effects of Quantum Fluctuations and the Action of Nonlinear Wigglers on Equilibrium Polarization Level". Nuovo Cimento 81B(1984)128-142.

[35] K. Yokoya: "Spin Chromaticity for Higher-Order Synchroton Resonances". Part. Acc. 13(1983)85-93.

8 Appendix

Date	Run	β^* [cm]	ν	P_{meas} [%]	P_∞ [%]	P^{HSM}_{meas} [%]	P^{HSM}_∞ [%]	$\#PU_{miss}$	Experiments
May, 25	1557	21	105.476	8	8	29	35 ± 4	10(13)	Solenoid spin matching: - ALEPH - DELPHI Harmonic Spin Matching. Damping wigglers.
May, 27	1568	21	≈ 101.5	21-16	21-16	27	69 ± 8	7(14)	Solenoid spin matching: - OPAL - L3 Harmonic Spin Matching. Damping wigglers.
June, 1	1578	5	≈ 103.5	4-12	4-12	-	-	-	Polarization in physics: - Physics tunes. - Two colliding beams. - Emittance wigglers.
June, 1/2	1579	21	101.485	-	-	9-27	61 ± 6	23(46)	Physics/Polarization tunes.
June, 3	1589	21	101.480	15	15	40	48 ± 5	22(28)	Energy calibration. Squeeze: beam lost.
June, 14	1616	var	101.455	-	-	30	46 ± 5	22(28)	Squeeze: β^* = 21 - 7 cm.
June, 14	1617	5	101.476	-	-	21	46 ± 5	22(28)	Betatron tune scan.
June, 20	1636	21	101.465	-	-	39	47 ± 3	24(30)	Systematic studies: - Polarimeter. - Energy calibration. - Harmonic Spin Matching.
June, 21	1637	5	101.483	-	-	29	-	23(35)	Energy calibration. Pretzel: beam lost.
August, 4/5	1734	21	101.35-101.48	-	-	24	43 ± 4	3(10)	Damping wiggler. Spin tune scan. Momentum compaction factor.
August, 29	1772	21	≈ 101.5	-	-	57	57 ± 3	4(14)	Energy calibration: - Dependence on temperature. Harmonic Spin Matching.
October, 11/12	1849	5	≈ 101.475	-	-	30	30	5(12)	Energy calibration: - Pretzel ON. - Measurement of tides. - Width of depolarizer res.. Damping wigglers: - Reduction of τ_p.

Table 4: *Overview on polarization experiments in 1993. If not explicitly mentioned Pretzel was off and only the electron beam was filled. For each run the maximum polarization level with (P^{HSM}_{meas}) and without (P_{meas}) Harmonic Spin Matching and the estimated asymptotic values are given. The number of missing pickups for orbit measurement $\#PU_{miss}$ is given for the arc and overall. This number must be compared to a total number of 240 pickups in the arcs and 508 pickups overall. The fills with more than 20 missing pickups in the arcs suffered from a broken BOM-station with 16 pickups on it. Apart from the first two runs all solenoids have been on and were spin matched.*